

# Discovery of Novel Benzimidazole and Indazole Analogues as Tubulin Polymerization Inhibitors with Potent Anticancer Activities

Yichang Ren,<sup>†</sup> Yuxi Wang,<sup>†</sup> Gang Li,<sup>†</sup> Zherong Zhang, Lingling Ma, Binbin Cheng, and Jianjun Chen\*



Cite This: *J. Med. Chem.* 2021, 64, 4498–4515



Read Online

ACCESS |



Metrics & More



Article Recommendations



Supporting Information



**ABSTRACT:** Novel indazole and benzimidazole analogues were designed and synthesized as tubulin inhibitors with potent antiproliferative activities. Among them, compound **12b** exhibited the strongest inhibitory effects on the growth of cancer cells with an average  $IC_{50}$  value of 50 nM, slightly better than colchicine. **12b** exhibited nearly equal potency against both, a paclitaxel-resistant cancer cell line (A2780/T,  $IC_{50} = 9.7$  nM) and the corresponding parental cell line (A2780S,  $IC_{50} = 6.2$  nM), thus effectively overcoming paclitaxel resistance *in vitro*. The crystal structure of **12b** in complex with tubulin was solved to 2.45 Å resolution by X-ray crystallography, and its direct binding was confirmed to the colchicine site. Furthermore, **12b** displayed significant *in vivo* antitumor efficacy in a melanoma tumor model with tumor growth inhibition rates of 78.70% (15 mg/kg) and 84.32% (30 mg/kg). Collectively, this work shows that **12b** is a promising lead compound deserving further investigation as a potential anticancer agent.

## INTRODUCTION

Microtubules, composed of  $\alpha$ -tubulin and  $\beta$ -tubulin heterodimers, are the key components of the cytoskeleton<sup>1</sup> and are of great importance for many cellular functions such as mitosis, cell motility, cell shape maintenance, intracellular transport, and cell signaling.<sup>2</sup> Owing to the polymerization dynamics of tubulin, microtubules are considered to be an important target for anticancer drugs, such as microtubule-targeting agents (MTAs),<sup>3,4</sup> which induce apoptosis by disrupting microtubule dynamics.<sup>5</sup> MTAs bind to one of the six binding sites on tubulin, the paclitaxel site,<sup>6,7</sup> the vinca site,<sup>8,9</sup> the laulimalide site,<sup>10,11</sup> the pironetin site,<sup>12</sup> the maytansine site,<sup>13,14</sup> and the colchicine site.<sup>15,16</sup> All currently marketed MTAs (*e.g.*, taxanes<sup>17</sup> and vinca alkaloids<sup>18</sup>) bind to the paclitaxel site or vinca site and are effective against a variety of cancers. Their clinical applications are often hindered by several drawbacks including low aqueous solubility, dose-limiting toxicity,<sup>19</sup> and multi-drug resistance (MDR).<sup>20–23</sup> Extensive research has shown that colchicine-binding site inhibitors (CBSIs) have the potential to overcome the abovementioned disadvantages associated with taxanes and vinca alkaloids, due to their structural simplicity, non-P-gp (P-glycoprotein) substrate nature, and reasonable pharmacokinetic properties.<sup>24–27</sup>

Although no CBSIs have been approved for clinical uses so far, several CBSIs (*e.g.*, BNC-105p, CA-4P, AVE8062, and VERU-111) are being actively investigated in clinical trials for the treatment of various cancers such as colon cancer, lung cancer, and prostate cancer ([www.clinicaltrials.gov](http://www.clinicaltrials.gov)). One of these investigational CBSIs, VERU-111 (in phase 2 clinical trial, NCT03752099), was originally discovered by us<sup>28</sup> and was found to have benign toxicity profiles ([www.verupharm.com](http://www.verupharm.com))<sup>29</sup> when compared to known tubulin inhibitors (*e.g.*, paclitaxel) targeting the taxane site. Thus, VERU-111 represents a promising CBSI with high therapeutic value in cancer treatment.

We have previously reported the discovery of several classes of CBSIs such as 2-aryl-4-benzoyl-imidazoles (ABI, **Figure 1**),<sup>28</sup> as mentioned above (code name VERU-111), 4-

Received: October 21, 2020

Published: March 31, 2021



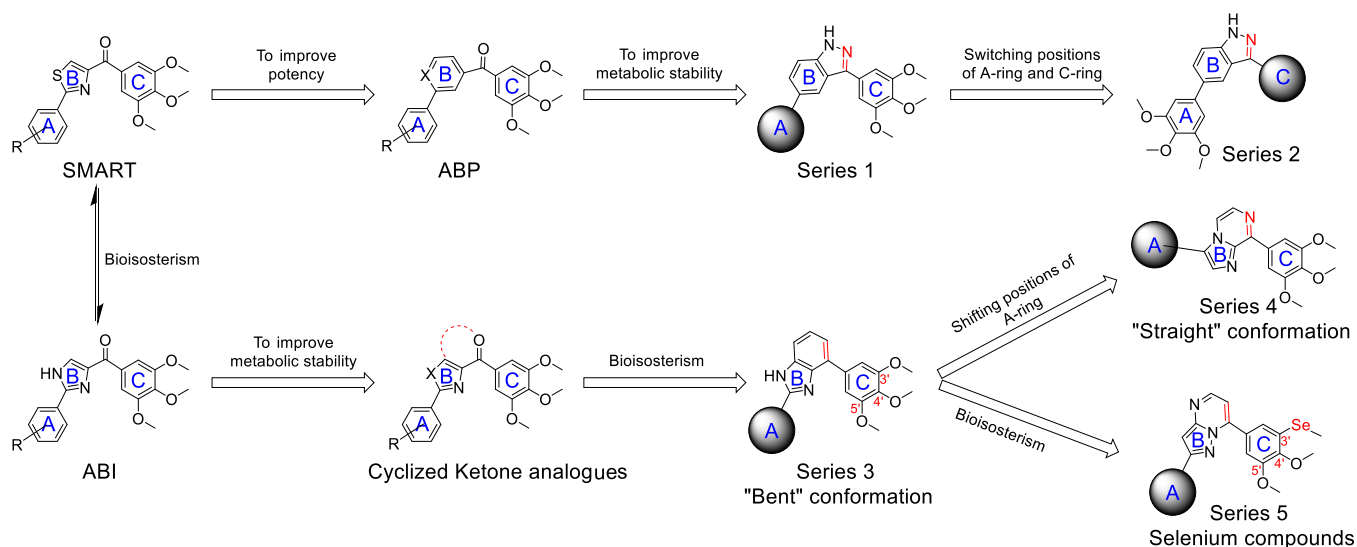
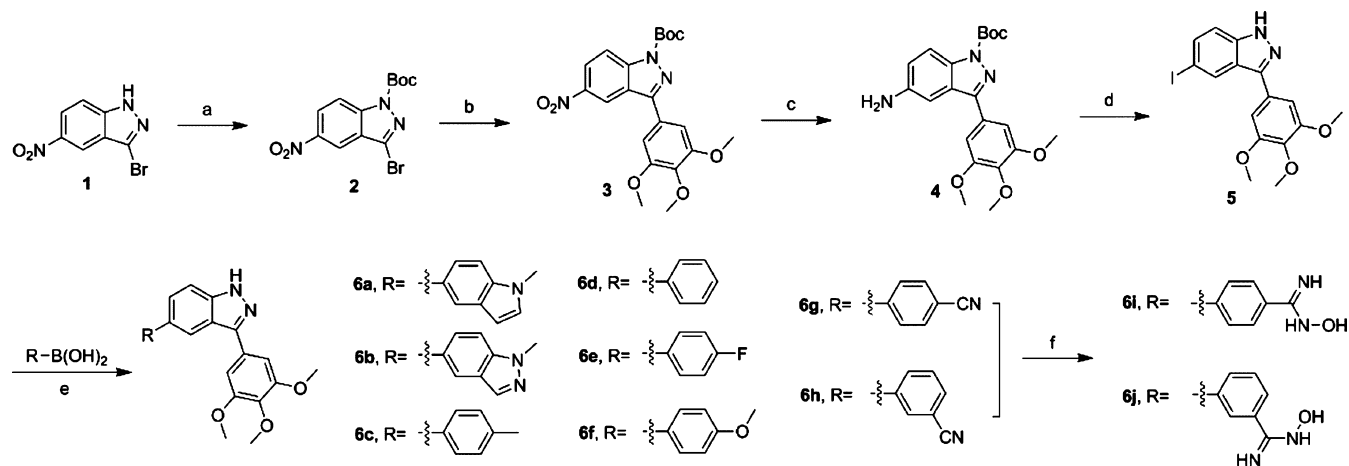


Figure 1. Design of target compounds by the ring-fusion strategy.

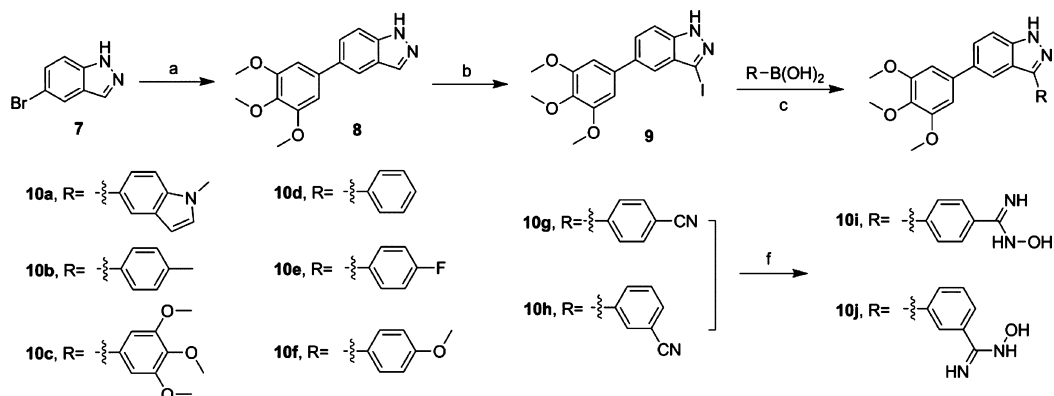
### Scheme 1. Synthesis of Series 1 Compounds (6a–j)<sup>a</sup>



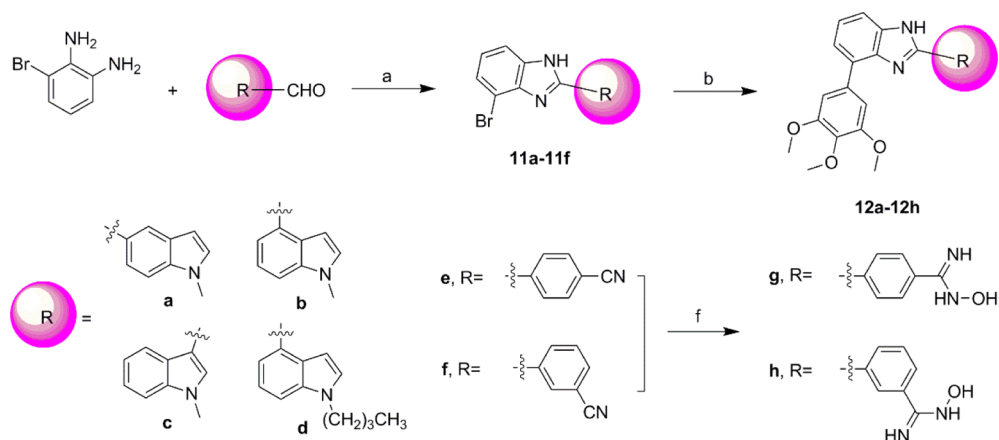
<sup>a</sup>Reagents and reaction conditions: (a) (Boc)<sub>2</sub>O, TEA, DMAP, and ACN; (b) 3,4,5-trimethoxyphenylboronic acid, PdCl<sub>2</sub>(dtbpf), Na<sub>2</sub>CO<sub>3</sub>, dioxane–H<sub>2</sub>O, 80 °C; (c) Pd/C, H<sub>2</sub> and MeOH–THF; (d) (i) NaNO<sub>2</sub>, 37% HCl, 0 °C; (ii) KI, 0 °C to room temperature, reflux; (e) PdCl<sub>2</sub>(dtbpf), Na<sub>2</sub>CO<sub>3</sub>, dioxane–H<sub>2</sub>O, 80 °C; and (f) NH<sub>2</sub>OHHCl, NaHCO<sub>3</sub>, EtOH, 65 °C.

substituted methoxybenzoyl-aryl-thiazoles (SMART),<sup>30</sup> and substituted-2-aryl imidazoles (SAI)<sup>31</sup> analogues. These CBSIs exhibited high *in vitro* antiproliferative activities and significant *in vivo* antitumor efficacy and were able to overcome P-gp-mediated MDR effectively. In spite of the excellent biological activities, the ABI and SMART analogues share a common structural feature, the carbonyl (ketone) group between the B-ring and C-ring (Figure 1), which is a metabolic soft spot and is susceptible to metabolic reduction by liver microsomes.<sup>32</sup> In order to improve the metabolic stability, we designed five series of compounds by incorporating the carbonyl group into a five-membered pyrazole ring (series 1 and 2: indazole analogues), a six-membered phenyl ring (series 3: benzimidazole analogues), and a six-membered pyrazine ring (series 4: pyrazine imidazole analogues) or a pyrimidine ring (series 5: selenium compounds based on the pyrazolo[1,5-*a*]pyrimidine scaffold). Previous co-crystal structures of an ABI compound in complex with tubulin showed that the binding pocket near the B-ring may accommodate a bulkier group,<sup>33,34</sup> and Li's group designed 6-aryl-2-benzoyl-pyridine/phenyl (ABP) analogues<sup>35</sup>

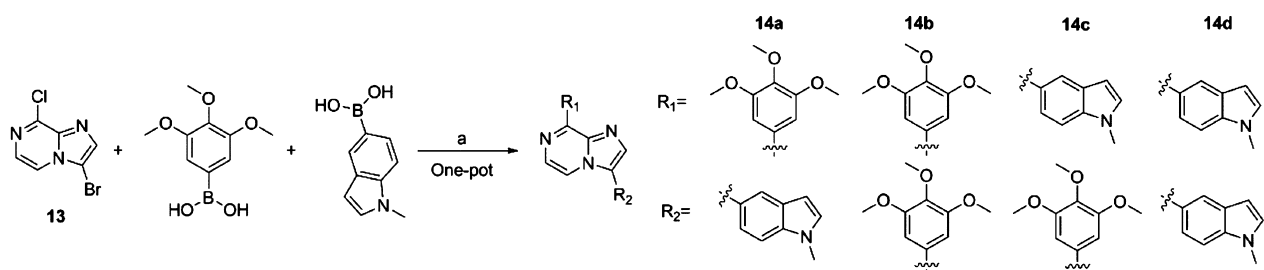
by replacing the five-membered imidazole B-ring of ABI with a six-membered phenyl or pyridine ring; ABP compounds exhibited high antiproliferative activities as tubulin inhibitors. Inspired by this, we designed series 1 by cyclizing the carbonyl moiety into a pyrazole ring to improve the metabolic stability. Series 2 was designed by switching the positions of the C-ring and A-ring of series 1. Series 3 ("bent" conformation) and series 4 ("straight" conformation) were designed by shifting the positions of the A-ring to explore the preferred conformations by the binding pocket.<sup>36</sup> Series 5 was designed by replacing the oxygen atom of the 3'-methoxy moiety with a selenium as selenium-containing compounds have been proven to be potent tubulin inhibitors.<sup>37,38</sup> In summary, the main strategy is to fuse the B-ring and cyclized ketone as the ring-fusion strategy is a common approach used in medicinal chemistry for drug design.<sup>39,40</sup> Here, we describe the design, synthesis, and biological evaluation of novel benzimidazole and indazole analogues as potential anticancer agents targeting tubulin polymerization.

Scheme 2. Synthesis of Series 2 Compounds (10a–j)<sup>a</sup>

<sup>a</sup>Reagents and reaction conditions: (a) 3,4,5-trimethoxyphenylboronic acid, PdCl<sub>2</sub>(dtbpf), Na<sub>2</sub>CO<sub>3</sub>, dioxane–H<sub>2</sub>O, 80 °C; (b) NIS and Actone; and (c) PdCl<sub>2</sub>(dtbpf), Na<sub>2</sub>CO<sub>3</sub>, dioxane–H<sub>2</sub>O, 80 °C.

Scheme 3. Synthesis of Series 3 Compounds (12a–h)<sup>a</sup>

<sup>a</sup>Reagents and reaction conditions: (a) TsOH, dioxane, 95 °C; (b) 3,4,5-trimethoxyphenylboronic acid, PdCl<sub>2</sub>(dtbpf), Na<sub>2</sub>CO<sub>3</sub>, dioxane–H<sub>2</sub>O, 80 °C.

Scheme 4. Synthesis of Series 4 Compounds (14a–d)<sup>a</sup>

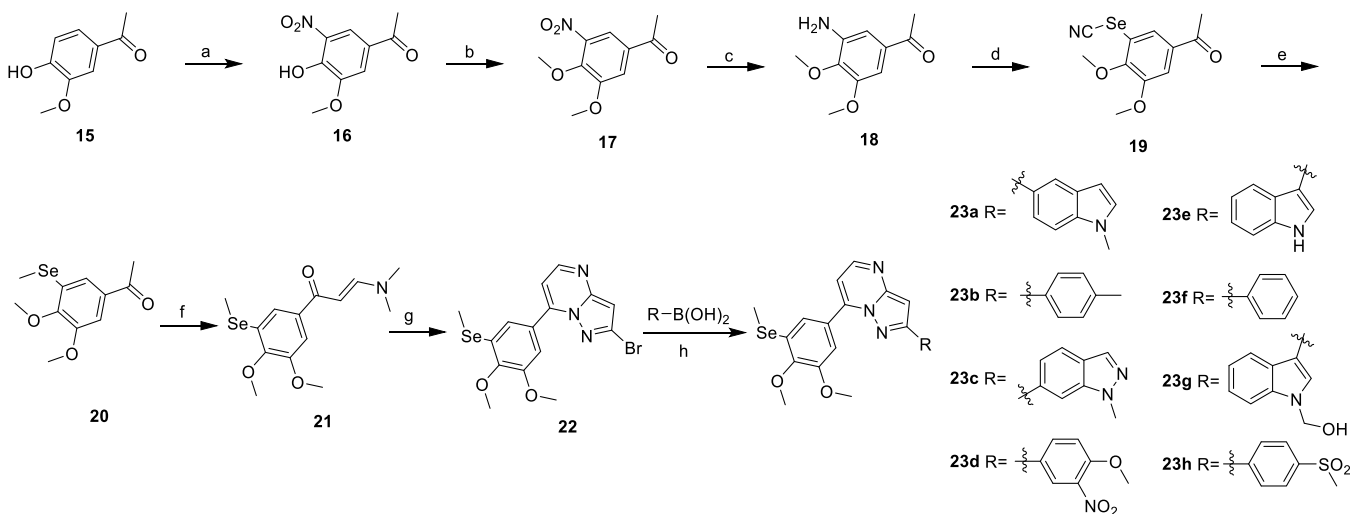
<sup>a</sup>Reagents and reaction conditions: (a) PdCl<sub>2</sub>(dtbpf), Na<sub>2</sub>CO<sub>3</sub>, dioxane–H<sub>2</sub>O, 80 °C.

## RESULTS AND DISCUSSION

**Chemistry.** The synthesis of series 1 compounds (6a–j) is illustrated in Scheme 1. 3-Bromo-5-nitro-1H-indazole (1) was protected by (Boc)<sub>2</sub>O to give intermediate 2, which underwent Suzuki reaction to yield intermediate 3. Intermediate 3 was reduced with hydrogen and Pd/C (10%) to generate intermediate 4, which was then converted to the 5-iodoindazole intermediate 5 under reported conditions.<sup>41</sup> Subsequently, intermediate 5 was coupled with a variety of arylboronic acid to produce compounds 6a–h. Treating

compounds 6g and 6h with hydroxylamine hydrochloride provided compounds 6i and 6j.

Series 2 compounds (10a–j) were synthesized and are outlined in Scheme 2. 5-Bromo-1H-indazole (7) was coupled with 3,4,5-trimethoxyphenylboronic acid to give the indazole compound 8 followed by an iodination reaction to produce 3-iodoindazole compound 9. Compound 9 underwent the Suzuki coupling reactions with various arylboronic acids to generate compounds 10a–h. Treating compounds 10g and 10h with hydroxylamine hydrochloride provided compounds 10i and 10j.

Scheme 5. Synthesis of Series 5 Selenium Compounds (23a–h)<sup>a</sup>

<sup>a</sup>Reagents and reaction conditions: (a) HNO<sub>3</sub>, AcOH, 3 h, rt; (b) dimethylsulfate, K<sub>2</sub>CO<sub>3</sub>, acetone, 48 h, 80 °C; (c) Pd/C, H<sub>2</sub>, CH<sub>3</sub>OH/THF, rt, overnight; (d) (i) HCl, H<sub>2</sub>O, NaNO<sub>2</sub>, 40 min, −5 °C; (ii) NaOAc, 30 min, 0 °C; (iii) KSeCN, 3 h, 0 °C, rt; (e) NaBH<sub>4</sub>, CH<sub>3</sub>I, EtOH, 10 min, rt; (f) *N,N*-dimethylformamide dimethyl acetal, DMF, 120 °C, 6 h; (g) 3-bromo-1*H*-pyrazol-5-amine, AcOH, 80 °C, 8 h; and (h) appropriate aryl boronic acid, Pd(dppf)Cl<sub>2</sub>, Na<sub>2</sub>CO<sub>3</sub> aq., DMF, 95 °C, 12 h.

Series 3 compounds (12a–h) were prepared and are illustrated in Scheme 3. 3-Bromo-1,2-benzenediamine was cyclized with different aldehydes to produce the benzimidazole intermediates 11a–f. Compounds 11a–f underwent Suzuki reaction with 3,4,5-trimethoxyphenylboronic acid to give compounds 12a–f. Treating compounds 12e and 12f with hydroxylamine hydrochloride provided compounds 12g and 12h.

Series 4 compounds (14a–d) were synthesized through a one-pot Suzuki reaction and are shown in Scheme 4.

Series 5 selenium compounds (23a–h) were prepared and are illustrated in Scheme 5. The intermediates 16–20 were prepared according to a reported procedure.<sup>38</sup> The selenium compound 20 was condensed with *N,N*-dimethylformamide dimethyl acetal at 120 °C to give compound 21, which was then stirred with 3-bromo-1*H*-pyrazol-5-amine at 80 °C to provide the key intermediate 22. Compound 22 underwent the Suzuki coupling reactions with various arylboronic acids to generate selenium compounds 23a–h.

**Biological Evaluation. *In Vitro* Antiproliferative Activities.** The newly synthesized compounds 6a–j, 10a–j, 12a–h, 14a–d, and 23a–h were evaluated for their *in vitro* cytotoxicity against four cancer cell lines by the MTT assay with colchicine as the positive control. As shown in Table 1, series 1 compounds, the indazole derivatives with a trimethoxyphenyl (TMP) moiety connected to the 3-position of indazole, exhibited moderate to high antiproliferative activities in general with IC<sub>50</sub> values in the low nanomolar to low micromolar range (e.g., 6a–j). Compound 6a with a 1-methyl-1*H*-indolyl moiety at the 5-position of indazole displayed the highest activity in this series with an average IC<sub>50</sub> of 81 nM. Replacing the 1-methyl-1*H*-indolyl moiety with an indazole (6b), a substituted phenyl (6c–h), or an *N*-hydroxycarbamimidoyl-phenyl (6i,j) led to diminished activities with average IC<sub>50</sub> values ranging from 0.22 μM (6c) to 6.6 μM (6j). Series 2 compounds (10a–j) lost their activities (IC<sub>50</sub> ~ 10 μM) due to the shift of the TMP group to the 5-position of indazole when compared with series 1 compounds (e.g., 10a vs 6a, 10b vs 6c, and 6d–j vs 10d–j). For series 3 compounds, the 1-

methyl-indole substituted benzimidazole analogues showed higher activities (average IC<sub>50</sub>s of 1.39, 0.05, and 0.70 μM for 12a, 12b, and 12c, respectively) than the corresponding 1-butyl-indole analogues (IC<sub>50</sub> > 10 μM for 12d). These results suggest that small substituents (e.g., methyl) are preferred over bulky functional groups (e.g., butyl) at *N*-1 of the indole ring (12a–c vs 12d). Compound 12b exhibited the highest activity with an average IC<sub>50</sub> of 50 nM which is slightly better than that of colchicine (IC<sub>50</sub> = 65 nM), indicating that the 4-substituted indolyl moiety is optimal for activity (12b vs 12a and 12c) in comparison to the 3- and 5-substituted indolyl groups. Series 4 compounds (14a–d) showed low activity (IC<sub>50</sub> > 10 μM) probably due to their “straight” conformation which is not preferred for binding to the colchicine-binding site in tubulin as compared to the “bent” conformation of series 3 compounds; similar results were also observed by Zhang’s group.<sup>36</sup> Series 5 compounds (23a–h) demonstrated high antiproliferative activities with IC<sub>50</sub> values in the low nanomolar to low micromolar range. In this series, compounds bearing an indolyl A-ring (e.g., 23a, 23e, and 23g) showed significantly better antiproliferative activities (IC<sub>50</sub> ranging from 91 to 856 nM) than those with a phenyl A-ring (e.g., 23d, 23f, and 23h, IC<sub>50</sub> ranging from 3 to 10 μM), consistent with our previous observations that the indolyl A-ring is optimal for activity.<sup>28</sup>

**Compound 12b Inhibited the Viability and Colony Formation of Cancer Cells.** To further validate the *in vitro* activities, the most potent compound 12b was chosen for the MTT and colony formation assay. On the MTT assay, compound 12b significantly decreased the viability of MCF-7, A549, HeLa, and B16-F10 cancer cells in a dose- and time-dependent manner (Figure 2A). In the colony formation assay using MCF-7 cells, compound 12b was able to suppress the formation of colonies in a dose-dependent manner, with the colony-forming ability of MCF-7 cells being totally suppressed after 24 h treatment with 500 nM of compound 12b (Figure 2B).

**Effects of Compound 12b on Paclitaxel-Resistant Cell Line.** Resistance to tubulin inhibitors such as paclitaxel and

Table 1. *In Vitro* Antiproliferative Activities of Target Compounds against Four Cancer Cell Lines<sup>a</sup>

Structure	Compound	R	IC <sub>50</sub> (μM)			
			MCF-7	A549	Hela	B16-F10
	<b>6a</b>	1-methyl-1H-indole-5-yl	0.026±0.001	0.093±0.012	0.141±0.008	0.064±0.007
	<b>6b</b>	1-methyl-1H-indazole-5-yl	0.360±0.026	6.216±0.630	2.023±0.039	2.622±0.159
	<b>6c</b>	4-methylphenyl	0.043±0.003	0.531±0.027	0.265±0.029	0.054±0.001
	<b>6d</b>	phenyl	0.245±0.061	0.445±0.023	0.547±0.081	0.394±0.044
	<b>6e</b>	4-fluorophenyl	0.606±0.102	0.759±0.073	0.926±0.034	0.635±0.068
	<b>6f</b>	4-methoxyphenyl	0.037±0.002	0.191±0.018	0.1324±0.026	0.1614±0.006
	<b>6g</b>	4-cyanophenyl	1.052±0.077	1.033±0.029	2.066±0.192	1.408±0.046
	<b>6h</b>	3-cyanophenyl	2.375±0.094	1.045±0.037	2.037±0.553	1.709±0.129
	<b>6i</b>	4-(N-hydroxycarbamimidoyl)	3.157±0.651	2.981±0.376	3.788±0.236	1.605±0.031
	<b>6j</b>	3-(N-hydroxycarbamimidoyl)	>10	6.254±0.310	4.680±0.603	8.028±0.427
	<b>10a</b>	1-methyl-1H-indole-5-yl	9.979±0.690	>10	8.030±0.232	9.256±0.318
	<b>10b</b>	4-methylphenyl	>10	>10	>10	>10
	<b>10c</b>	3,4,5-trimethoxyphenyl	>10	7.899±0.524	8.617±0.144	7.265±0.094
	<b>10d</b>	phenyl	>10	>10	>10	>10
	<b>10e</b>	4-fluorophenyl	>10	>10	>10	>10
	<b>10f</b>	4-methoxyphenyl	>10	>10	>10	>10
	<b>10g</b>	4-cyanophenyl	>10	>10	>10	>10
	<b>10h</b>	3-cyanophenyl	>10	>10	>10	>10
	<b>10i</b>	4-(N-hydroxycarbamimidoyl)	>10	>10	>10	>10
	<b>10j</b>	3-(N-hydroxycarbamimidoyl)	>10	>10	>10	>10
	<b>12a</b>	1-methyl-1H-indole-5-yl	0.700±0.102	2.601±0.241	1.540±0.034	0.746±0.086
	<b>12b</b>	1-methyl-1H-indole-4-yl	0.018±0.004	0.085±0.007	0.068±0.010	0.029±0.004
	<b>12c</b>	1-methyl-1H-indole-3-yl	0.176±0.003	1.008±0.052	0.981±0.252	0.631±0.015
	<b>12d</b>	1-butyl-1H-indole-4-yl	>10	>10	>10	>10
	<b>12e</b>	4-cyanophenyl	>10	>10	>10	>10
	<b>12f</b>	3-cyanophenyl	>10	>10	6.685±0.423	6.187±0.196
	<b>12g</b>	4-(N-hydroxycarbamimidoyl)	>10	>10	>10	>10
	<b>12h</b>	3-(N-hydroxycarbamimidoyl)	>10	>10	>10	>10
	<b>14a</b>	1-methyl-1H-indol-5-yl	>10	>10	>10	>10
	<b>14b</b>	3,4,5-trimethoxyphenyl	>10	>10	>10	>10
	<b>14c</b>	3,4,5-trimethoxyphenyl	>10	>10	>10	>10
	<b>14d</b>	1-methyl-1H-indol-5-yl	>10	>10	>10	>10
	<b>23a</b>	1-methyl-1H-indole-5-yl	0.123±0.023	0.372±0.011	0.091±0.009	0.126±0.017
	<b>23b</b>	4-methylphenyl	0.168±0.006	0.231±0.041	0.211±0.022	0.443±0.059
	<b>23c</b>	1-methyl-1H-indazol-6-yl	1.184±0.083	1.246±0.126	2.177±0.226	3.701±0.111
	<b>23d</b>	4-methoxy-3-nitrophenyl	6.194±0.088	>10	6.333±0.387	7.952±0.174
	<b>23e</b>	1H-indol-3-yl	0.349±0.055	0.360±0.073	0.312±0.015	0.662±0.031
	<b>23f</b>	phenyl	3.161±0.312	>10	6.252±0.247	7.125±0.192
	<b>23g</b>	1-hydroxymethyl-1H-indole-3-yl	0.313±0.008	0.224±0.011	0.279±0.029	0.856±0.018
	<b>23h</b>	4-(methylsulfonyl)phenyl	3.155±0.562	6.978±0.269	4.587±0.137	8.524±0.624
	Colchicine		0.021±0.006	0.108±0.011	0.051±0.004	0.083±0.006

<sup>a</sup>Cells were exposed to different concentrations of compounds continuously for 48 h prior to determination of cell viability by the MTT assay. IC<sub>50</sub> values are presented as the mean ± SD (standard error) of at least three independent experiments.

colchicine is a major obstacle impeding the clinical use of these agents. In our previous work, the ABI analogues demonstrated the ability to circumvent paclitaxel resistance effectively. We hypothesized that the cyclized ketone analogues designed on the basis of the ABI scaffold would maintain the ability to overcome paclitaxel resistance. To verify this hypothesis, we

examined the antiproliferative activity of compound **12b** in a paclitaxel-resistant cancer cell line (A2780/T) and the corresponding parental cells (A2780S), with paclitaxel and colchicine as positive controls. In the A2780/T cell line, P-gp is overexpressed, which may represent the primary mechanism of resistance to paclitaxel.<sup>42</sup> As shown in Table 2, compound

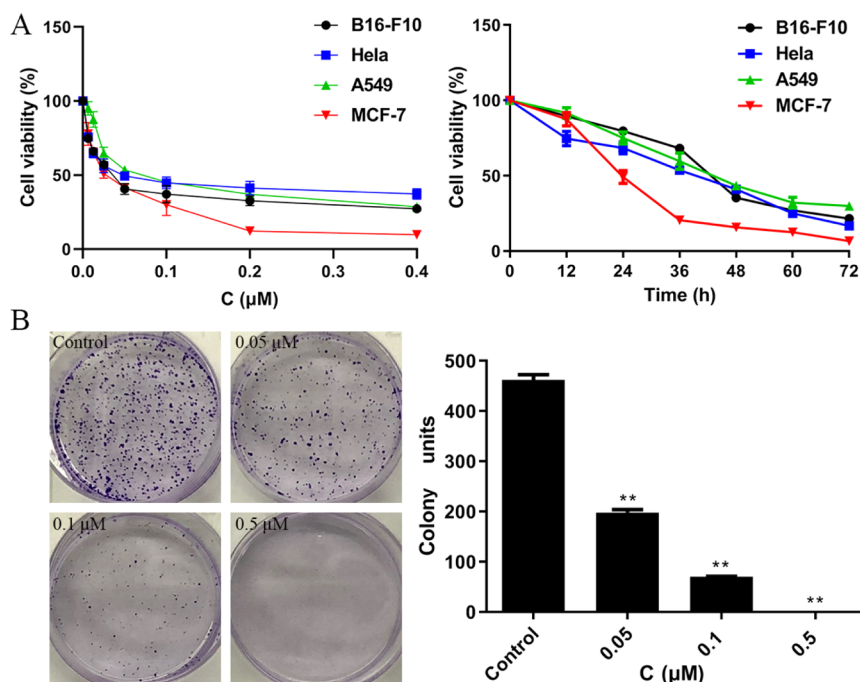


**Figure 2.** Growth inhibitory effects of compound **12b** on cancer cells. (A) Four cancer cell lines, MCF-7, A549, HeLa, and B16-F10 were treated with the indicated concentration of compound **12b** for 48 h (left panel) or compound **12b** (100 nM) for the indicated time (right panel). Cell viability was determined by MTT assays. (B) Number of colonies was counted after treating MCF-7 cells with the indicated concentration of compound **12b** for 24 h ( $n = 3$ ,  $**P < 0.05$  vs DMSO control).

**Table 2. Drug Tolerances of Compound 12b against A2780/T**

drug	IC <sub>50</sub> (nM)		RI <sup>a</sup>
	A2780/T	A2780S	
<b>12b</b>	9.7 ± 4.1	6.2 ± 2.1	1.6
paclitaxel	3164.0 ± 147.1	7.5 ± 3.4	421.8
colchicine	783.8 ± 62.7	16.7 ± 6.6	46.9

<sup>a</sup>Resistant index: (IC of drug-resistant cancer cell)/(IC of parental cancer cell).

**12b** was nearly equally potent against both the parental (A2780S) and its paclitaxel-resistant cell line (A2780/T) with IC values of 6.2 and 9.7 nM, respectively, and a resistance index (RI) of 1.6. While paclitaxel and colchicine showed low nanomolar potency (7.5 and 16.7 nM) in the parental A2780S cells, the activity was significantly lower (3164.0 and 783.8

nM) in the A2780/T cell line with RIs of 421.8 and 46.9, respectively.

Because a colony formation assay has been generally used to predict the therapeutic efficacy of a drug to solid tumors, we therefore performed it to examine the effect of compound **12b** on paclitaxel-resistant cells (A2780/T). As shown in Figure S1 (Supporting Information), compound **12b** suppressed the formation of A2780/T colonies in a dose-dependent manner, and even at the lowest tested concentration of 10 nM, **12b** was able to effectively inhibit A2780/T colony formation. However, paclitaxel could not inhibit the formation of A2780/T colonies even at a high concentration of 100 nM. These results suggest that compound **12b** is probably not a substrate for P-gp and thus could overcome P-gp-mediated MDR *in vitro* in A2780/T cells.

*In Vitro Tubulin Polymerization Assay and Binding Kinetics to Tubulin.* Based on the high *in vitro* antiproliferative activities, we further evaluated the inhibitory effects of

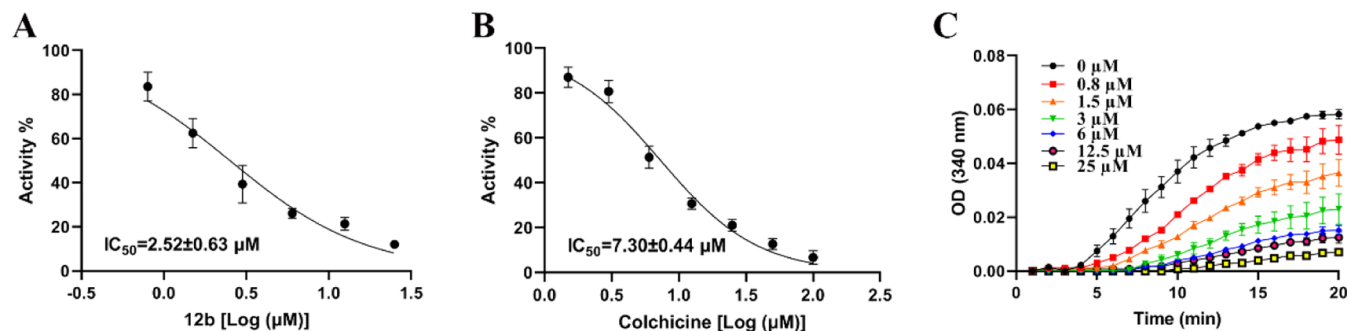


**Figure 3.** Inhibition of tubulin polymerization *in vitro*. (A) Inhibition of tubulin polymerization by compound **12b**. (B) Inhibition of tubulin polymerization by colchicine. (C) Compound **12b** exhibited a dose-dependent inhibition of tubulin polymerization. Data are expressed as mean ± standard deviation from three independent experiments.

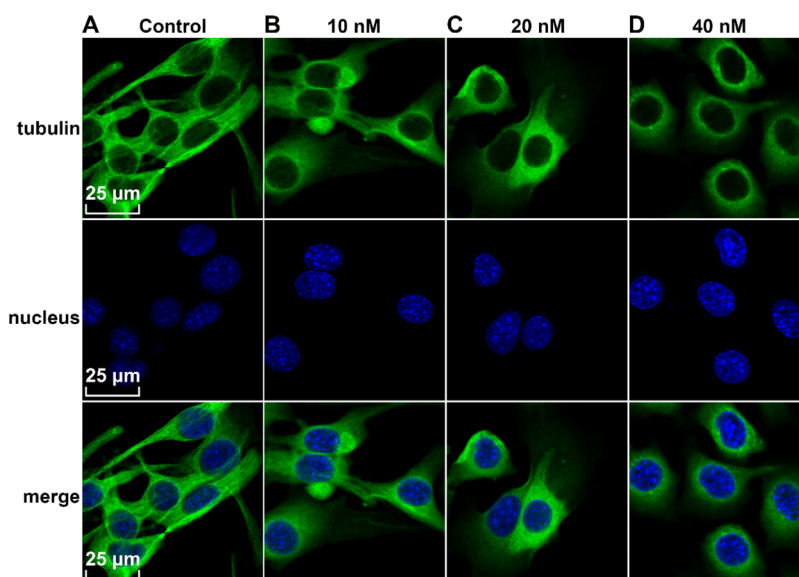


**Figure 4.** Effects of compound **12b** on microtubules. B16-F10 cells were treated with vehicle control 0.1% DMSO (A), compound **12b** (10 nM) (B), compound **12b** (20 nM) (C), and compound **12b** (40 nM) (D) for 6 h. Microtubules were visualized with an anti- $\beta$ -tubulin antibody (green), and the cell nucleus was visualized with DAPI (blue). Fluorescence images were collected by a LSM 880 laser confocal microscope (Carl Zeiss, Germany).

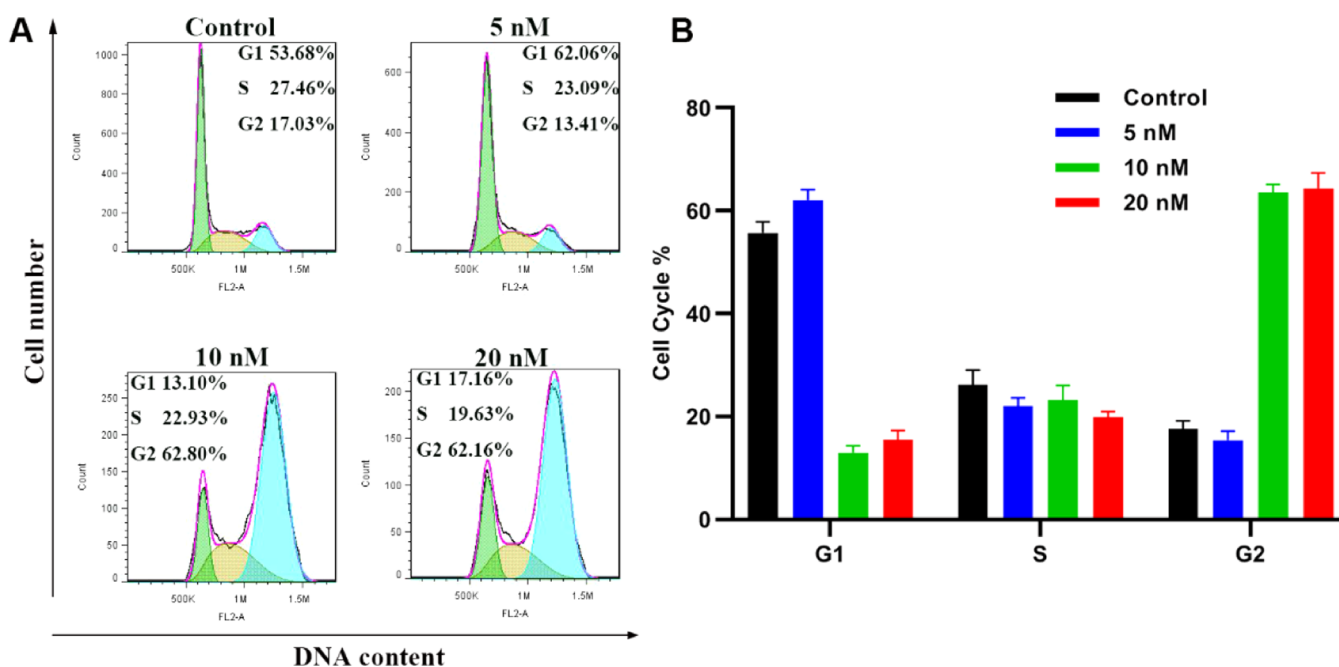


**Figure 5.** Cell cycle arrest induced by compound **12b**. (A) Compound **12b** induced G2/M arrest in MCF-7 cells. MCF-7 cells were incubated with varying concentrations of compound **12b** (5, 10, and 20 nM) for 48 h. The percentages of cells in different phases of the cell cycle were analyzed by FlowJo 7.6.1. (B) Histograms display the percentage of cell cycle distribution after treatment with compound **12b**. Data are expressed as mean  $\pm$  standard deviation from three independent experiments.

compound **12b** on tubulin polymerization with colchicine as a positive control. As shown in Figure 3, compound **12b** potently inhibited tubulin polymerization with an  $IC_{50}$  of  $2.52 \pm 0.63 \mu\text{M}$  (Figure 3A), which is better than that of colchicine ( $IC_{50} = 7.30 \pm 0.44 \mu\text{M}$ , Figure 3B). Furthermore, compound **12b** inhibited tubulin polymerization in a dose-dependent manner (Figure 3C). In addition, we also performed an surface plasmon resonance (SPR) experiment to explore the binding affinity of our compounds to tubulin with colchicine as a control. As shown in Figure S2 (Supporting Information),

compound **12b** dose dependently binds to tubulin with a  $K_D$  of  $12.7 \mu\text{M}$ , similar to that of colchicine ( $K_D = 25.4 \mu\text{M}$ ). These results indicate that **12b** could bind to tubulin at a similar magnitude to that of colchicine.

**Antimicrotubule Effects in B16-F10 Cells.** The inhibitory effect of compound **12b** on microtubule organization was further studied in B16-F10 cells by immunofluorescence staining. As illustrated in Figure 4, in the control experiment [dimethyl sulfoxide (DMSO)], the microtubule networks appeared in a normal arrangement with slim and fibrous

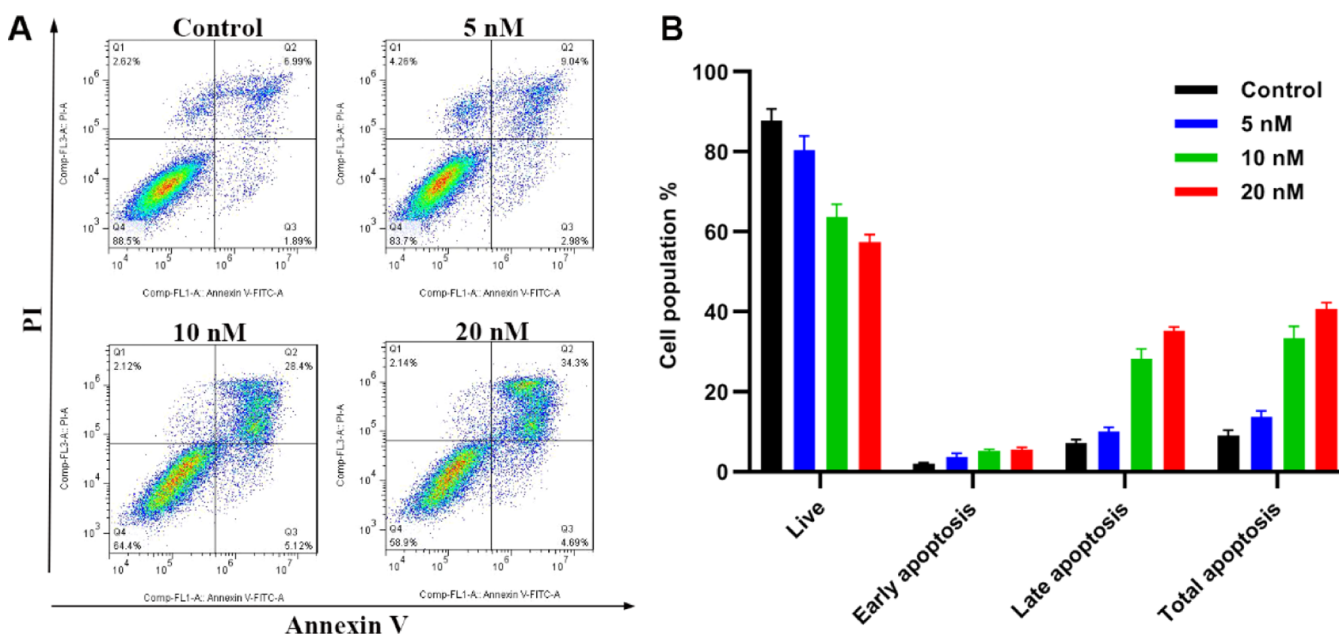


**Figure 6.** Effects of compound **12b** on cancer cell apoptosis. (A) Compound **12b** induced apoptosis in MCF-7 cells. MCF-7 cells were exposed to increasing concentrations of compound **12b** (5, 10, and 20 nM) for 48 h. The percentages of cells in each stage of cell apoptosis were quantified by flow cytometry: necrosis cells (upper left quadrant); late apoptotic cells (upper right quadrant); live cells (bottom left quadrant); and early apoptotic cells (bottom right quadrant). (B) Histograms displayed the percentage of cell cycle distribution after treatment with compound **12b**. Data are expressed as mean  $\pm$  standard deviation from three independent experiments.

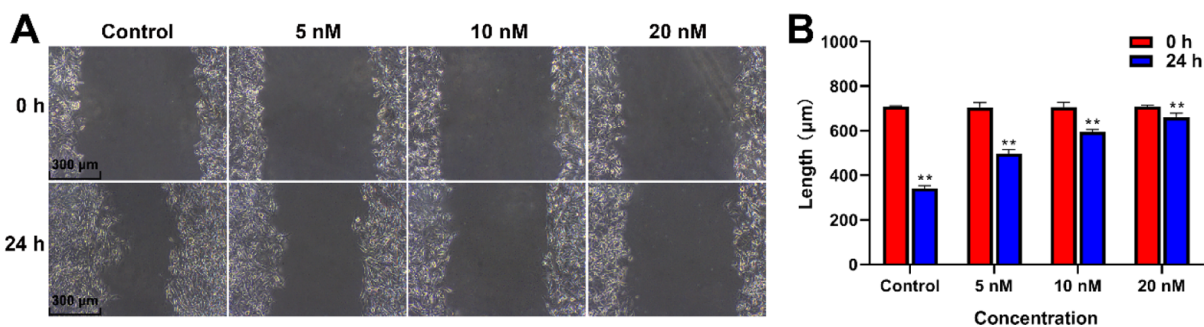


**Figure 7.** Effects on the B16-F10 cell migration. (A) Representative images of wound area in a wound healing assay. Images were obtained at 0 and 24 h after treatment with 0, 5, 10, and 20 nM of compound **12b**. (B) Histograms display the length of the scratches at 0 and 24 h after treatments with 0, 5, 10, and 20 nM of compound **12b** ( $n = 3$ ,  $**P < 0.05$  vs DMSO control).

microtubules (green) wrapped around the cell nucleus (blue). However, the microtubule networks in cytosol were disrupted when cells were exposed to compound **12b** (10, 20, and 40 nM) for 6 h. These results suggest that compound **12b** may induce a dose-dependent collapse of the microtubule networks.

**Cell Cycle Analysis.** Tubulin polymerization inhibitors have been previously reported to disrupt cell mitosis and induce cell cycle arrest.<sup>43</sup> Thus, flow cytometry analysis was performed to examine the effects of compound **12b** on the cell cycle of MCF-7 cells. As shown in Figure 5A,B, treatment of cells with compound **12b** for 48 h caused a significant accumulation of MCF-7 cells in the G2/M phase with the percentage of cells distributed in the G2/M phase of around 62% at 10 and 20 nM, as compared to the control group (17%).

**Analysis of Cancer Cell Apoptosis.** Knowing that mitotic arrest of tumor cells by tubulin polymerization inhibitors is generally associated with cellular apoptosis, an annexin V-FITC and propidium iodide (PI) assay of compound **12b** was performed with MCF-7 cells, in order to assess whether compound **12b** could induce cancer cell apoptosis. As shown

in Figure 6A,B, after treating MCF-7 cells with increasing concentrations of compound **12b** (5, 10, and 20 nM) for 48 h, the total numbers of early (annexin-V+/PI-) and late (annexin-V+/PI+) apoptotic cells were  $13.71 \pm 1.49$ ,  $33.28 \pm 3.12$ , and  $40.66 \pm 1.61\%$ , respectively. These results confirmed that **12b** could induce efficient apoptosis of MCF-7 cells.

**Inhibition of Cancer Cell Migration.** It is implicated that tubulin and microtubule played an important role in cell migration and motility. Therefore, we performed a wound healing assay in order to confirm the effects of compound **12b** in cell migration *via* microtubule destabilization. B16-F10 cells were treated with 0, 5, 10, and 20 nM of compound **12b** for 24 h. The result of the wound closure is shown in Figure 7. The control cells were able to migrate into the wound channel, recovering  $51.92 \pm 2.02\%$  of the area. Treating with 5, 10, or 20 nM of compound **12b**, B16-F10 cells only migrated into  $29.42 \pm 4.93$ ,  $15.68 \pm 2.03$ , and  $6.60 \pm 2.09\%$  of the wound area, respectively. Obviously, displaying that the migration of

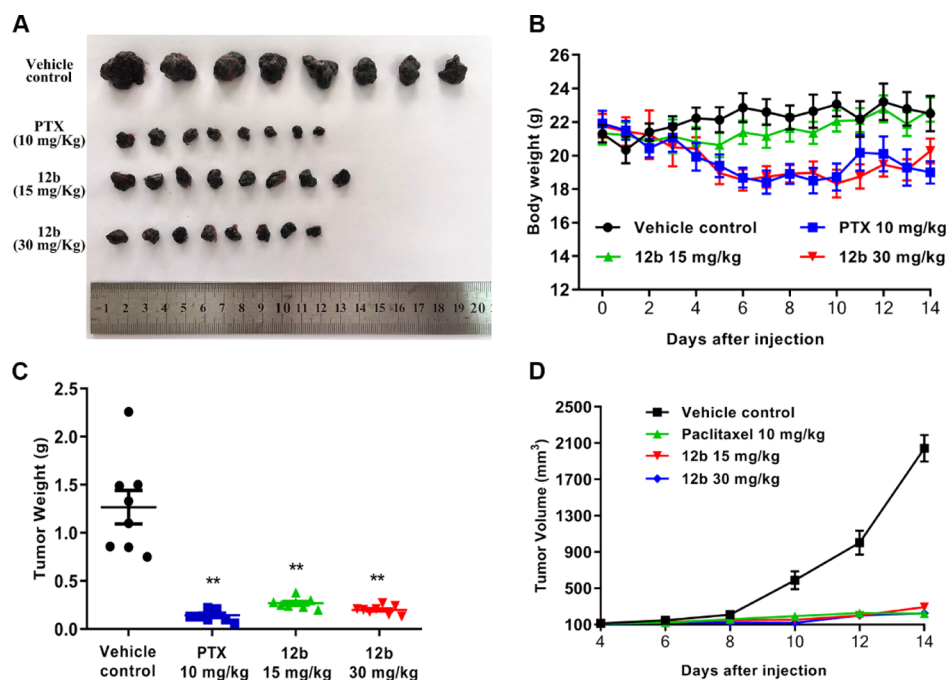


**Figure 8.** Compound **12b** inhibits melanoma tumor growth *in vivo*. After being administered with vehicle, PTX (10 mg/kg per days), compound **12b** (15 mg/kg per day), and compound **12b** (30 mg/kg per day) for 14 days, the mice were sacrificed, and the tumors were weighed. (A) Images of tumors from mice at 14 days after initiation of treatment. (B) Body weight changes of mice during treatment. (C) Weight of the excised tumors of each group.  $**P < 0.05$  vs control group. (D) Tumor volume changes of mice during treatment.

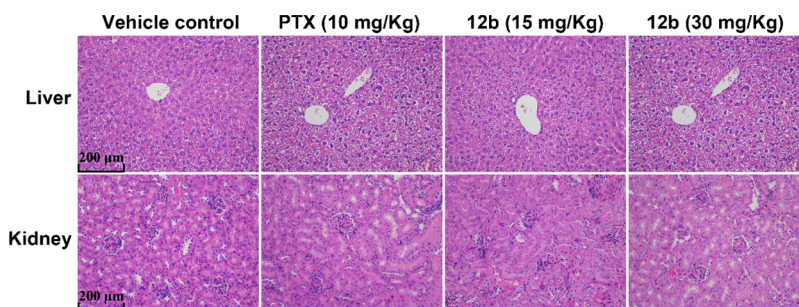


**Figure 9.** Pathological sections of major tissues (liver and kidney) were obtained from mice bearing melanoma tumors. Organs were stained with H&E, and the representative images are captured.

cancer cells was suppressed by compound **12b** in a dose-dependent manner.

**In vivo Antitumor Efficacy.** The *in vivo* antitumor efficacy of compound **12b** was further evaluated in the mice melanoma tumor model, established by subcutaneous inoculation of B16-F10 cells into the mice. BALB/c mice bearing melanoma tumors were treated with vehicle control, paclitaxel (PTX, 10 mg/kg), and compound **12b** (15, 30 mg/kg) *via* i.p. injection every once a day for 14 days. As shown in Figure 8, compound **12b** demonstrated significant *in vivo* antitumor efficacy with tumor growth inhibition (TGI) of 78.70 and 84.32% at 15 and 30 mg/kg, respectively, slightly less than that of PTX (88.66%) at 10 mg/kg. In addition, compound **12b** did not cause an obvious body weight loss at 15 mg/kg, indicating that the compound was well-tolerated at low doses (Figure 8B). Furthermore, the hematoxylin and eosin (H&E) staining of liver and kidney showed that compound **12b** had no significant toxic effects on the major organs of mice (Figure 9).

**X-ray Structures of Compound 12b in Complex with Tubulin.** To reveal the binding interactions of compound **12b** with tubulin, we determined the crystal structures of T2R-TTL

[composed of two  $\alpha/\beta$  tubulin dimers, the stathmin-like protein RB3, and tubulin tyrosine ligase (TTL)] in complex with compound **12b** at a resolution of 2.45 Å (PDB code: 7DBA). The X-ray diffraction data and structure refinement statistics are shown in Table 3.

As expected, compound **12b** occupies the colchicine-binding site at the interface of the  $\alpha$ - and  $\beta$ -tubulin opposite to the GTP molecule (Figure 10A). There is a hydrogen bond formed between compound **12b** and  $\beta$ -tubulin: the nitrogen atom of the imidazole ring of compound **12b** and the  $-\text{OH}$  in  $\beta$ -Asn258 (Figure 10B–D). In addition, compound **12b** is wrapped firmly in the colchicine-binding site with a hydrophobic “sandwich” formed by the side-chains of  $\beta$ -Cys241,  $\beta$ -Leu248, and  $\beta$ -Lys352 from one side and that of  $\beta$ -Lys254 from the other side. The observed hydrogen bond and the strong hydrophobic interaction between the ligand and tubulin may explain the high activity of **12b**.

## CONCLUSIONS

In summary, we designed, synthesized, and bioevaluated novel indazole and benzimidazole analogues as tubulin inhibitors,

Table 3. X-ray Data Collection and Refinement Statistics

T2R-TTL-12b (PDB code: 7DBA)	
data collection	
space group	P121221
cell dimensions	
unit cell (Å)	105.4 158.9 181.6
unit cell (°)	90.0, 90, 90
wavelength (Å)	0.9793
resolution (Å)	31.3–2.45
$R_{\text{merge}}$	0.141 (0.80)
$CC_{1/2}$	97.7 (74.1)
I/ $\sigma$	12.3 (1.5)
completeness (%)	99.9 (99.6)
redundancy	6.5 (6.4)
structure refinement	
number of measured reflections	717,379
number of unique reflections	110,366
$R_{\text{work}}/R_{\text{free}}$ (%)	18.92/22.82
no. atoms	18,135
protein	17,520
water	433
ligand	182
average B value (Å <sup>2</sup> )	53.35
protein	53.67
others	43.18
r.m.s. deviations	
bonds (Å)	0.01
angle (°)	0.83
Ramachandran plot statistics (%)	
most favorable	96.92
allowed	3.08
disallowed	0

targeting the colchicine-binding site. These compounds showed high *in vitro* antiproliferative activities with  $IC_{50}$  values in the nanomolar range. Among them, compound **12b** displayed the highest activity against a panel of cancer cell lines with an average  $IC_{50}$  value 50 nM, which is slightly better than colchicine. Compound **12b** exhibited nearly equal activity against both, a paclitaxel-resistant cancer cell line (A2780/T) and the corresponding parental cell line (A2780S). Thus, compound **12b** can effectively overcome paclitaxel resistance *in vitro*. Mechanism studies revealed that compound **12b** inhibited tubulin polymerization, arrested the cell cycle in the G2/M phase, and induced apoptosis in MCF-7 cells. The crystal structure of **12b** in complex with tubulin was solved to 2.45 Å resolution by X-ray crystallography and confirmed its direct binding to the colchicine site. In addition, compound **12b** displayed significant *in vivo* antitumor efficacy in a melanoma tumor model with a significant TGI of 78.70% (15 mg/kg) and 84.32% (30 mg/kg) without apparent toxicity. Collectively, this work shows that compound **12b** is a promising lead compound deserving further investigation as a potential anticancer agent.

## EXPERIMENTAL SECTION

**General Methods.** Unless otherwise specified, all chemicals and reagents were obtained from commercial suppliers and were used without further purification. The reference compounds (paclitaxel and colchicine) were acquired from InvivoChem (Libertyville, IL 60048, USA). <sup>1</sup>H and <sup>13</sup>C NMR spectra were recorded on a Bruker Avance at 400 MHz, using CDCl<sub>3</sub> or DMSO-*d*<sub>6</sub> as solvent and tetramethylsilane as internal standard. Chemical shifts are reported in parts per million

(ppm). Multiplicities are reported as follows: singlet (s), doublet (d), triplet (t), quartet (q), double doublet (dd), and multiplet (m). Compound purities were estimated by reversed phase C18 high-performance liquid chromatography, with UV detection at 254 nm. The major peak area of each tested compound was  $\geq 95\%$  of the combined total peak area. High-resolution mass spectrometry (HRMS) was obtained on a Micromass Q-TOF mass spectrometer. Column chromatography was carried out using commercially available silica gel (200–300 mesh) under pressure.

**Synthesis of Intermediate 2.** To a solution of 3-bromo-5-nitro-1H-indazole (**1**) (1.0 g, 4.13 mmol) and (Boc)<sub>2</sub>O (947 mg, 4.34 mmol) in 20 mL of acetonitrile (ACN) were added 4-dimethylaminopyridine (DMAP) (202 mg, 1.65 mmol) and TEA (triethyl amine, 859  $\mu$ L, 6.20 mmol). The mixture was stirred at room temperature overnight. The solvent was removed *in vacuo*, and the residue was diluted by H<sub>2</sub>O and extracted with EtOAc (3  $\times$  20 mL). The combined organic layer was then washed with brine, dried over anhydrous Na<sub>2</sub>SO<sub>4</sub>, and concentrated *in vacuo* to provide the crude product, which was directly subjected to silica gel column chromatography eluted with petroleum PE/EtOAc (9/1, v/v) to give intermediate **2** as a white solid (1.1 g, 79.2%). <sup>1</sup>H NMR (400 MHz, CDCl<sub>3</sub>):  $\delta$  8.57 (d,  $J$  = 2.1 Hz, 1H), 8.45 (dd,  $J$  = 9.2, 2.1 Hz, 1H), 8.31 (d,  $J$  = 9.2 Hz, 1H), 1.73 (s, 9H).

**Synthesis of Intermediate 3.** To a solution of intermediate **2** (1.0 g, 2.92 mmol) in 18 mL of dioxane and 2 mL of H<sub>2</sub>O were added (3,4,5-trimethoxyphenyl)boronic acid (682 mg, 3.21 mmol), Na<sub>2</sub>CO<sub>3</sub> (620 mg, 5.85 mmol), and catalytic equivalent of PdCl<sub>2</sub>(dtbpf). The mixture was stirred at 80 °C under a nitrogen atmosphere for 4 h. Then, the solvent was removed *in vacuo*, and the residue was diluted by H<sub>2</sub>O and extracted with EtOAc (3  $\times$  20 mL). The combined organic layer was then washed with brine, dried over anhydrous Na<sub>2</sub>SO<sub>4</sub>, and concentrated *in vacuo* to provide the crude product, which was directly subjected to silica gel column chromatography eluted with petroleum PE/EtOAc (4/1, v/v) to give intermediate **3** as yellow oil (693 mg, 55.9%). <sup>1</sup>H NMR (400 MHz, CDCl<sub>3</sub>):  $\delta$  8.87 (d,  $J$  = 1.8 Hz, 1H), 8.45 (dd,  $J$  = 9.3, 2.1 Hz, 1H), 8.34 (d,  $J$  = 9.2 Hz, 1H), 7.16 (s, 2H), 3.98 (s, 6H), 3.94 (s, 3H), 1.77 (s, 9H).

**Synthesis of Intermediate 4.** To a stirred solution of intermediate **3** (500 mg, 1.16 mmol) in 5 mL of THF and 5 mL of MeOH was added Pd/C (10%) to hydrogenate for 24 h. The mixture was then filtered, and the filtrate was concentrated to dryness *in vacuo*. The residue was purified by silica gel column chromatography eluted with PE/EtOAc (1/1, v/v) to give intermediate **4** as yellow oil (440 mg, 94.6%). <sup>1</sup>H NMR (400 MHz, CDCl<sub>3</sub>):  $\delta$  7.97 (d,  $J$  = 8.9 Hz, 1H), 7.18–7.13 (m, 3H), 6.97 (dd,  $J$  = 8.9, 2.1 Hz, 1H), 3.95 (s, 6H), 3.91 (s, 3H), 1.73 (s, 9H).

**Synthesis of Intermediate 5.** Intermediate **4** (200 mg, 0.501 mmol) was suspended in 37% HCl (5 mL) at 0 °C. An ice-cold solution of NaNO<sub>2</sub> (52 mg, 0.751 mmol) in H<sub>2</sub>O (2.5 mL) was added dropwise, and the resulting solution was stirred at 0–5 °C for 10 min. An ice-cold suspension of KI (104 mg, 0.626 mmol) in 37% HCl (2.5 mL) was added dropwise. The mixture was stirred at room temperature for 10 min, then at reflux for 3 h, and at room temperature for 16 h. NaOH solution was added to adjust the mixture to neutral. Then, the mixture was filtered, and the filter residue was purified by silica gel column chromatography eluted with PE/EtOAc (2/1, v/v) to give intermediate **5** as a white solid (85 mg, 41.4%). <sup>1</sup>H NMR (400 MHz, CDCl<sub>3</sub>):  $\delta$  7.95 (d,  $J$  = 1.2 Hz, 1H), 7.45 (d,  $J$  = 8.8 Hz, 1H), 7.39 (dd,  $J$  = 8.8, 1.8 Hz, 1H), 7.12 (s, 2H), 3.97 (s, 6H), 3.93 (s, 3H).

**General Procedures for the Preparation of Compounds 6a–6h.** To a solution of intermediate **5** (20 mg, 0.039 mmol) in 4.5 mL of dioxane and 0.5 mL of H<sub>2</sub>O were added arylboronic acid (0.043 mmol), Na<sub>2</sub>CO<sub>3</sub> (9 mg, 0.078 mmol), and catalytic equivalent of PdCl<sub>2</sub>(dtbpf). The mixture was stirred at 80 °C under a nitrogen atmosphere for 4 h. Then, the solvent was removed *in vacuo*, and the residue was diluted by H<sub>2</sub>O and extracted with EtOAc (3  $\times$  10 mL). The combined organic layer was then washed with brine, dried over anhydrous Na<sub>2</sub>SO<sub>4</sub>, and concentrated *in vacuo* to provide the crude product, which was directly subjected to silica gel column

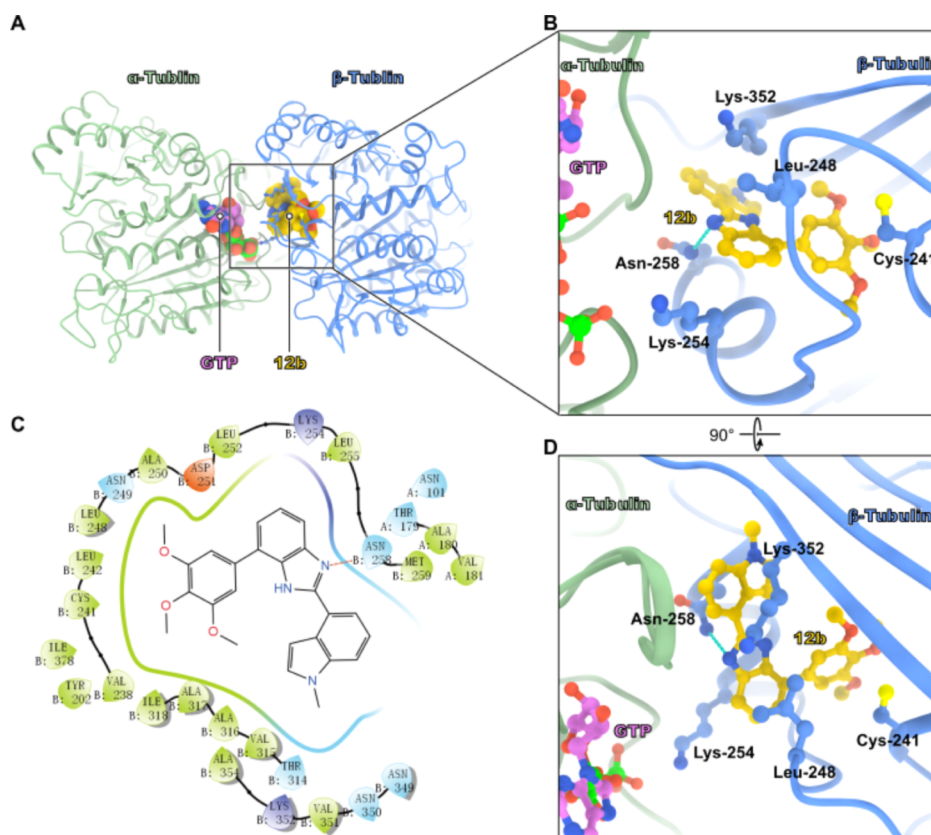


**Figure 10.** T2R-TTL crystal in complex with compound 12b (PDB code: 7DBA). (A) Overall structure of the  $\alpha/\beta$ -tubulin and 12b complex. Compound 12b and GTP are shown in violet and yellow spheres, respectively. (B) 3D detailed interactions between compound 12b and tubulin at the colchicine-binding domain. (C) 2D detailed interactions between compound 12b and tubulin at the colchicine-binding domain. (D) 90° clockwise rotation of corresponding structures along the  $x$ -axis. Oxygen and nitrogen atoms are colored red and blue, respectively. Hydrogen bond is indicated in green dashed line.

chromatography eluted with petroleum PE/EtOAc (2/1, v/v) to give corresponding pure compounds 6a–6h.

**3-(3,4,5-Trimethoxyphenyl)-5-(1-methyl-1H-indole-5-yl)-1H-indazole (6a).** The compound was obtained as a white solid; yield: 34.3%. m.p. 190.1–191.5 °C.  $^1\text{H NMR}$  (400 MHz,  $\text{CDCl}_3$ ):  $\delta$  8.21 (s, 1H), 7.89 (s, 1H), 7.78 (d,  $J = 8.6$  Hz, 1H), 7.58–7.52 (m, 2H), 7.44 (d,  $J = 8.5$  Hz, 1H), 7.28 (s, 1H), 7.27 (s, 1H), 7.13 (d,  $J = 2.9$  Hz, 1H), 6.57 (d,  $J = 2.9$  Hz, 1H), 5.32 (s, 1H), 3.97 (d,  $J = 5.3$  Hz, 9H), 3.86 (s, 3H).  $^{13}\text{C NMR}$  (101 MHz,  $\text{CDCl}_3$ ):  $\delta$  153.81, 146.31, 140.99, 136.91, 136.25, 133.32, 130.07, 130.04, 129.78, 129.36, 129.21, 128.04, 121.80, 119.78, 119.15, 110.23, 109.74, 105.11, 101.44, 61.15, 56.48, 33.12. HRMS  $m/z$ : calcd for  $\text{C}_{25}\text{H}_{23}\text{N}_3\text{O}_3$  [ $\text{M} + \text{H}$ ] $^+$ , 413.1739; found, 414.1818.

**3-(3,4,5-Trimethoxyphenyl)-5-(1-methyl-1H-indazole-5-yl)-1H-indazole (6b).** The compound was obtained as a white solid; yield: 40.8%. m.p. 192.4–193.6 °C.  $^1\text{H NMR}$  (400 MHz,  $\text{CDCl}_3$ ):  $\delta$  8.19 (s, 1H), 8.07 (s, 1H), 7.96 (s, 1H), 7.75 (d,  $J = 8.7$  Hz, 1H), 7.72 (d,  $J = 8.7$  Hz, 1H), 7.61 (d,  $J = 8.6$  Hz, 1H), 7.52 (d,  $J = 8.7$  Hz, 1H), 7.25 (s, 2H), 4.15 (s, 3H), 3.99 (s, 6H), 3.96 (d,  $J = 0.7$  Hz, 3H).  $^{13}\text{C NMR}$  (101 MHz,  $\text{CDCl}_3$ ):  $\delta$  153.65, 146.17, 140.92, 139.22, 138.38, 135.54, 134.65, 134.37, 133.02, 128.97, 127.56, 126.67, 124.65, 121.61, 119.29, 119.18, 110.33, 109.32, 105.01, 60.96, 56.31, 35.61. HRMS  $m/z$ : calcd for  $\text{C}_{24}\text{H}_{22}\text{N}_4\text{O}_3$  [ $\text{M} + \text{H}$ ] $^+$ , 414.1692; found, 415.1779.

**3-(3,4,5-Trimethoxyphenyl)-5-(4-methylphenyl)-1H-indazole (6c).** The compound was obtained as a white solid; yield: 45.7%. m.p. 164.8–165.0 °C.  $^1\text{H NMR}$  (400 MHz,  $\text{CDCl}_3$ ):  $\delta$  8.16 (s, 1H), 7.72 (dd,  $J = 8.7, 1.4$  Hz, 1H), 7.60 (d,  $J = 8.8$  Hz, 1H), 7.56 (d,  $J = 8.1$  Hz, 2H), 7.31 (d,  $J = 7.9$  Hz, 2H), 7.23 (s, 2H), 6.11 (s, 1H), 3.99 (s, 6H), 3.96 (s, 3H), 2.44 (s, 3H). HRMS  $m/z$ : calcd for  $\text{C}_{23}\text{H}_{22}\text{N}_2\text{O}_3$  [ $\text{M} + \text{H}$ ] $^+$ , 374.1630; found, 375.1740.

**3-(3,4,5-Trimethoxyphenyl)-5-phenyl-1H-indazole (6d).** The compound was obtained as a white solid; yield: 59.7%. m.p. 161.2–161.8 °C.  $^1\text{H NMR}$  (400 MHz,  $\text{CDCl}_3$ ):  $\delta$  8.16 (s, 1H), 7.69 (dd,  $J = 8.7, 1.5$  Hz, 1H), 7.64 (d,  $J = 7.3$  Hz, 2H), 7.54 (d,  $J = 8.7$  Hz, 1H), 7.47 (t,  $J = 7.6$  Hz, 2H), 7.37 (t,  $J = 7.3$  Hz, 1H), 7.22 (s, 2H), 3.96 (s, 6H), 3.94 (s, 3H). HRMS  $m/z$ : calcd for  $\text{C}_{22}\text{H}_{20}\text{N}_2\text{O}_3$  [ $\text{M} + \text{H}$ ] $^+$ , 360.1474; found, 361.1599.

**3-(3,4,5-Trimethoxyphenyl)-5-(4-fluorophenyl)-1H-indazole (6e).** The compound was obtained as a white solid; yield: 51.3%. m.p. 162.4–162.9 °C.  $^1\text{H NMR}$  (400 MHz,  $\text{CDCl}_3$ ):  $\delta$  8.09 (s, 1H), 7.64 (dd,  $J = 8.7, 1.4$  Hz, 1H), 7.60–7.55 (m, 3H), 7.20 (s, 2H), 7.16 (t,  $J = 8.7$  Hz, 2H), 3.96 (s, 6H), 3.94 (s, 3H). HRMS  $m/z$ : calcd for  $\text{C}_{22}\text{H}_{19}\text{FN}_2\text{O}_3$  [ $\text{M} + \text{H}$ ] $^+$ , 378.1380; found, 379.1484.

**3-(3,4,5-Trimethoxyphenyl)-5-(4-methoxyphenyl)-1H-indazole (6f).** The compound was obtained as a white solid; yield: 61.5%. m.p. 158.1–158.8 °C.  $^1\text{H NMR}$  (400 MHz,  $\text{CDCl}_3$ ):  $\delta$  8.10 (s, 1H), 7.64 (dd,  $J = 8.7, 1.4$  Hz, 1H), 7.56 (d,  $J = 8.7$  Hz, 2H), 7.49 (d,  $J = 8.7$  Hz, 1H), 7.22 (s, 2H), 7.01 (d,  $J = 8.7$  Hz, 2H), 3.96 (s, 6H), 3.94 (s, 3H), 3.87 (s, 3H). HRMS  $m/z$ : calcd for  $\text{C}_{23}\text{H}_{22}\text{N}_2\text{O}_4$  [ $\text{M} + \text{H}$ ] $^+$ , 390.1580; found, 391.1690.

**3-(3,4,5-Trimethoxyphenyl)-5-(4-cyanophenyl)-1H-indazole (6g).** The compound was obtained as a white solid; yield: 52.6%. m.p. 184.8–185.6 °C.  $^1\text{H NMR}$  (400 MHz, DMSO):  $\delta$  8.30 (s, 1H), 7.98 (d,  $J = 8.4$  Hz, 2H), 7.91 (d,  $J = 8.4$  Hz, 2H), 7.79 (d,  $J = 8.7$  Hz, 1H), 7.71 (d,  $J = 8.7$  Hz, 1H), 7.23 (s, 2H), 3.89 (s, 6H), 3.73 (s, 3H). HRMS  $m/z$ : calcd for  $\text{C}_{23}\text{H}_{19}\text{N}_3\text{O}_3$  [ $\text{M} + \text{H}$ ] $^+$ , 385.1426; found, 386.1519.

**3-(3,4,5-Trimethoxyphenyl)-5-(3-cyanophenyl)-1H-indazole (6h).** The compound was obtained as a white solid; yield: 49.3%. m.p. 181.1–181.8 °C.  $^1\text{H NMR}$  (400 MHz, DMSO):  $\delta$  8.29 (s, 1H), 8.25 (s, 1H), 8.11 (d,  $J = 8.0$  Hz, 1H), 7.79 (t,  $J = 7.5$  Hz, 2H), 7.71–7.65 (m,  $J = 15.5, 8.0$  Hz, 2H), 7.23 (s, 2H), 3.90 (s, 6H), 3.74 (s, 3H).

HRMS  $m/z$ : calcd for  $C_{23}H_{19}N_3O_3$   $[M + H]^+$ , 385.1426; found, 386.1515.

**General Procedures for the Preparation of Compounds 6i and 6j.** To a solution of compound **6g** or **6h** (27 mg, 0.070 mmol) in 5 mL of anhydrous EtOH were added hydroxylamine hydrochloride (8 mg, 0.105 mmol) and  $NaHCO_3$  (18 mg, 0.210 mmol). The mixture was stirred at 65 °C under a nitrogen atmosphere for 6 h. Then, the solvent was removed *in vacuo*, and the residue was subjected to silica gel column chromatography eluted with petroleum PE/EtOAc (1/2, v/v) to give corresponding pure compound **6i** or **6j**.

**3-(3,4,5-Trimethoxyphenyl)-5-[4-(*N*-hydroxycarbamimidoyl)]-1H-indazole (6i).** The compound was obtained as a white solid; yield: 43.4%. m.p. 174.7–175.9 °C.  $^1H$  NMR (400 MHz, DMSO):  $\delta$  13.27 (s, 1H), 9.65 (s, 1H), 8.23 (s, 1H), 7.77 (s, 4H), 7.74 (s, 1H), 7.68 (d,  $J = 8.7$  Hz, 1H), 7.24 (s, 2H), 5.83 (s, 2H), 3.90 (s, 6H), 3.74 (s, 3H). HRMS  $m/z$ : calcd for  $C_{23}H_{22}N_4O_4$   $[M + H]^+$ , 418.1641; found, 419.1729.

**3-(3,4,5-Trimethoxyphenyl)-5-[3-(*N*-hydroxycarbamimidoyl)]-1H-indazole (6j).** The compound was obtained as a white solid; yield: 40.9%. m.p. 172.8–173.9 °C.  $^1H$  NMR (400 MHz, DMSO):  $\delta$  13.27 (s, 1H), 9.64 (s, 1H), 8.28 (s, 1H), 8.04 (s, 1H), 7.77 (t,  $J = 6.5$  Hz, 2H), 7.71–7.66 (m, 2H), 7.47 (t,  $J = 7.7$  Hz, 1H), 7.25 (s, 2H), 5.93 (s, 2H), 3.91 (s, 6H), 3.74 (s, 3H). HRMS  $m/z$ : calcd for  $C_{23}H_{22}N_4O_4$   $[M + H]^+$ , 418.1641; found, 419.1733.

**Synthesis of Intermediate 8.** To a solution of 5-bromo-1H-indazole (**7**) (1.0 g, 5.08 mmol) in 27 mL of dioxane and 3 mL of  $H_2O$  were added (3,4,5-trimethoxyphenyl)boronic acid (1.18 g, 5.58 mmol), catalytic equivalent of  $PdCl_2(dtbpf)$ , and  $Na_2CO_3$  (1.08 g, 10.15 mmol). The mixture was stirred at 80 °C under a nitrogen atmosphere for 4 h. Then, the solvent was removed *in vacuo*, and the residue was diluted with  $H_2O$  and extracted with EtOAc (3  $\times$  20 mL). The combined organic layer was then washed with brine, dried over anhydrous  $Na_2SO_4$ , and concentrated *in vacuo* to provide the crude product, which was directly subjected to silica gel column chromatography eluted with petroleum PE/EtOAc (4/1, v/v) to give intermediate **8** as a white solid (995 mg, 68.9%).  $^1H$  NMR (400 MHz,  $CDCl_3$ ):  $\delta$  8.15 (s, 1H), 7.91 (s, 1H), 7.63 (d,  $J = 8.7$  Hz, 1H), 7.56 (d,  $J = 8.6$  Hz, 1H), 6.82 (s, 2H), 3.95 (s, 6H), 3.91 (s, 3H).

**Synthesis of Intermediate 9.** To a stirred solution of intermediate **8** (800 mg, 2.81 mmol) in 20 mL of acetone was added NIS (*N*-iodosuccinimide, 760 mg, 3.38 mmol). After stirring at room temperature overnight, the solvent was removed *in vacuo*, and the residue was diluted by  $H_2O$  and extracted with EtOAc (3  $\times$  20 mL). The combined organic layer was then washed with brine, dried over anhydrous  $Na_2SO_4$ , and concentrated *in vacuo* to provide the crude product, which was directly subjected to silica gel column chromatography eluted with petroleum PE/EtOAc (2/1, v/v) to give intermediate **9** as a white solid (666 mg, 57.8%).  $^1H$  NMR (400 MHz,  $CDCl_3$ ):  $\delta$  7.67 (dd,  $J = 8.7, 1.5$  Hz, 1H), 7.62 (s, 1H), 7.55 (d,  $J = 8.7$  Hz, 1H), 6.82 (s, 2H), 3.96 (s, 6H), 3.91 (s, 3H).

**General Procedures for the Preparation of Compounds 10a–h.** To a solution of intermediate **9** (30 mg, 0.073 mmol) in 4.5 mL of dioxane and 0.5 mL of  $H_2O$  were added arylboronic acid (0.080 mmol),  $Na_2CO_3$  (16 mg, 0.146 mmol), and catalytic equivalent of  $PdCl_2(dtbpf)$ . The mixture was stirred at 80 °C under a nitrogen atmosphere for 4 h. Then, the solvent was removed *in vacuo*, and the residue was diluted by  $H_2O$  and extracted with EtOAc (3  $\times$  10 mL). The combined organic layer was then washed with brine, dried over anhydrous  $Na_2SO_4$ , and concentrated *in vacuo* to provide the crude product, which was directly subjected to silica gel column chromatography eluted with petroleum PE/EtOAc (2/1, v/v) to give corresponding pure compounds **10a–10h**.

**3-(1-Methyl-1H-indole-5-yl)-5-(3,4,5-trimethoxyphenyl)-1H-indazole (10a).** The compound was obtained as a white solid; yield: 36.8%. m.p. 182.4–183.8 °C.  $^1H$  NMR (400 MHz,  $CDCl_3$ ):  $\delta$  8.23 (s, 1H), 8.20 (s, 1H), 7.87 (d,  $J = 8.4$  Hz, 1H), 7.62 (d,  $J = 8.6$  Hz, 1H), 7.53 (d,  $J = 8.6$  Hz, 1H), 7.49 (d,  $J = 8.4$  Hz, 1H), 7.13 (d,  $J = 3.0$  Hz, 1H), 6.82 (s, 2H), 6.60 (d,  $J = 2.8$  Hz, 1H), 3.94 (s, 6H), 3.91 (s, 3H), 3.86 (s, 3H). HRMS  $m/z$ : calcd for  $C_{25}H_{23}N_3O_3$   $[M + H]^+$ , 413.1739; found, 414.1837.

**3-(4-Methylphenyl)-5-(3,4,5-trimethoxyphenyl)-1H-indazole (10b).** The compound was obtained as a white solid; yield: 48.2%. m.p. 176.0–176.7 °C.  $^1H$  NMR (400 MHz,  $CDCl_3$ ):  $\delta$  8.15 (d,  $J = 7.8$  Hz, 1H), 7.92 (d,  $J = 8.0$  Hz, 1H), 7.77–7.61 (m, 2H), 7.60–7.53 (m, 1H), 7.38 (d,  $J = 7.9$  Hz, 1H), 7.34 (d,  $J = 7.6$  Hz, 1H), 6.84 (s, 2H), 3.99 (s, 3H), 3.97 (s, 3H), 3.94 (s, 3H), 2.47 (s, 3H). HRMS  $m/z$ : calcd for  $C_{23}H_{22}N_2O_3$   $[M + H]^+$ , 374.1630; found, 375.1743.

**3-(3,4,5-Trimethoxyphenyl)-5-(3,4,5-trimethoxyphenyl)-1H-indazole (10c).** The compound was obtained as a white solid; yield: 50.6%. m.p. 183.5–184.8 °C.  $^1H$  NMR (400 MHz,  $CDCl_3$ ):  $\delta$  8.13 (s, 1H), 7.67 (dd,  $J = 8.6, 1.2$  Hz, 1H), 7.55 (d,  $J = 8.7$  Hz, 1H), 7.25 (s, 2H), 6.84 (s, 2H), 4.04–3.95 (m, 15H), 3.94 (s, 3H). HRMS  $m/z$ : calcd for  $C_{25}H_{26}N_2O_6$   $[M + H]^+$ , 450.1791; found, 451.1888.

**3-Phenyl-5-(3,4,5-trimethoxyphenyl)-1H-indazole (10d).** The compound was obtained as a white solid; yield: 66.7%. m.p. 162.1–163.0 °C.  $^1H$  NMR (400 MHz,  $CDCl_3$ ):  $\delta$  8.13 (s, 1H), 8.02 (d,  $J = 7.2$  Hz, 2H), 7.61 (dd,  $J = 8.6, 1.1$  Hz, 1H), 7.56 (t,  $J = 7.5$  Hz, 2H), 7.50–7.44 (m, 2H), 6.81 (s, 2H), 3.95 (s, 6H), 3.92 (s, 3H). HRMS  $m/z$ : calcd for  $C_{22}H_{20}N_2O_3$   $[M + H]^+$ , 360.1474; found, 361.1591.

**3-(4-Fluorophenyl)-5-(3,4,5-trimethoxyphenyl)-1H-indazole (10e).** The compound was obtained as a white solid; yield: 51.4%. m.p. 158.2–158.6 °C.  $^1H$  NMR (400 MHz,  $CDCl_3$ ):  $\delta$  8.06 (s, 1H), 8.00–7.95 (m, 2H), 7.64 (dd,  $J = 8.7, 1.5$  Hz, 1H), 7.54 (d,  $J = 8.7$  Hz, 1H), 7.22 (t,  $J = 8.4$  Hz, 2H), 6.80 (s, 2H), 3.95 (s, 6H), 3.91 (s, 3H). HRMS  $m/z$ : calcd for  $C_{22}H_{19}FN_2O_3$   $[M + H]^+$ , 378.1380; found, 379.1499.

**3-(4-Methoxyphenyl)-5-(3,4,5-trimethoxyphenyl)-1H-indazole (10f).** The compound was obtained as a white solid; yield: 59.1%. m.p. 155.7–156.6 °C.  $^1H$  NMR (400 MHz,  $CDCl_3$ ):  $\delta$  8.09 (s, 1H), 7.94 (d,  $J = 8.8$  Hz, 2H), 7.61 (dd,  $J = 8.7, 1.4$  Hz, 1H), 7.49 (d,  $J = 8.7$  Hz, 1H), 7.08 (d,  $J = 8.8$  Hz, 2H), 6.81 (s, 2H), 3.95 (s, 6H), 3.91 (s, 3H), 3.90 (s, 3H). HRMS  $m/z$ : calcd for  $C_{23}H_{22}N_2O_4$   $[M + H]^+$ , 390.1580; found, 391.1716.

**3-(4-Cyanophenyl)-5-(3,4,5-trimethoxyphenyl)-1H-indazole (10g).** The compound was obtained as a white solid; yield: 50.8%. m.p. 192.3–194.0 °C.  $^1H$  NMR (400 MHz,  $CDCl_3$ ):  $\delta$  8.14 (d,  $J = 8.5$  Hz, 2H), 8.08 (s, 1H), 7.82 (d,  $J = 8.5$  Hz, 2H), 7.68 (dd,  $J = 8.7, 1.4$  Hz, 1H), 7.62 (d,  $J = 8.6$  Hz, 1H), 6.80 (s, 2H), 3.95 (s, 6H), 3.92 (s, 3H). HRMS  $m/z$ : calcd for  $C_{23}H_{19}N_3O_3$   $[M + H]^+$ , 385.1426; found, 386.1513.

**3-(3-Cyanophenyl)-5-(3,4,5-trimethoxyphenyl)-1H-indazole (10h).** The compound was obtained as a white solid; yield: 46.7%. m.p. 190.6–192.3 °C.  $^1H$  NMR (400 MHz,  $CDCl_3$ ):  $\delta$  8.30 (s, 1H), 8.25 (d,  $J = 7.8$  Hz, 1H), 8.05 (s, 1H), 7.72–7.06 (m, 4H), 6.80 (s, 2H), 3.96 (s, 6H), 3.92 (s, 3H). HRMS  $m/z$ : calcd for  $C_{23}H_{19}N_3O_3$   $[M + H]^+$ , 385.1426; found, 386.1501.

**General Procedures for the Preparation of Compounds 10i and 10j.** To a solution of compound **10g** or **10h** (27 mg, 0.070 mmol) in 5 mL of anhydrous EtOH were added hydroxylamine hydrochloride (8 mg, 0.105 mmol) and  $NaHCO_3$  (18 mg, 0.210 mmol). The mixture was stirred at 65 °C under a nitrogen atmosphere for 6 h. Then, the solvent was removed *in vacuo*, and the residue was subjected to silica gel column chromatography eluted with petroleum PE/EtOAc (1/2, v/v) to give corresponding pure compound **10i** or **10j**.

**3-[4-(*N*-Hydroxycarbamimidoyl)]-5-(3,4,5-trimethoxyphenyl)-1H-indazole (10i).** The compound was obtained as a white solid; yield: 41.9%. m.p. 182.1–183.0 °C.  $^1H$  NMR (400 MHz, DMSO):  $\delta$  13.34 (s, 1H), 9.71 (s, 1H), 8.22 (s, 1H), 8.07 (d,  $J = 8.3$  Hz, 2H), 7.84 (d,  $J = 8.3$  Hz, 2H), 7.72 (d,  $J = 8.6$  Hz, 1H), 7.66 (d,  $J = 8.7$  Hz, 1H), 6.96 (s, 2H), 3.88 (s, 6H), 3.70 (s, 3H). HRMS  $m/z$ : calcd for  $C_{23}H_{22}N_4O_4$   $[M + H]^+$ , 418.1641; found, 419.1721.

**3-[3-(*N*-Hydroxycarbamimidoyl)]-5-(3,4,5-trimethoxyphenyl)-1H-indazole (10j).** The compound was obtained as a white solid; yield: 55.6%. m.p. 179.9–180.6 °C.  $^1H$  NMR (400 MHz,  $CDCl_3$ ):  $\delta$  8.26 (s, 1H), 7.99 (s, 1H), 7.95 (d,  $J = 7.5$  Hz, 1H), 7.63 (d,  $J = 7.6$  Hz, 1H), 7.53–7.41 (m, 3H), 6.72 (s, 2H), 5.24 (s, 2H), 3.87 (s, 9H). HRMS  $m/z$ : calcd for  $C_{23}H_{22}N_4O_4$   $[M + H]^+$ , 418.1641; found, 419.1741.

**General Procedures for the Preparation of Intermediates 11a–11f.** To a solution of 3-bromo-1,2-benzenediamine (100 mg,

0.535 mmol) in 5 mL of dioxane were added aldehyde (0.641 mmol) and TsOH (0.080 mmol). The mixture was stirred at 95 °C under a nitrogen atmosphere for 48 h. Then, the solvent was removed *in vacuo*, and the residue was diluted by H<sub>2</sub>O and extracted with EtOAc (3 × 10 mL). The combined organic layer was then washed with brine, dried over anhydrous Na<sub>2</sub>SO<sub>4</sub>, and concentrated *in vacuo* to provide the crude product, which was directly subjected to silica gel column chromatography eluted with petroleum PE/EtOAc (2/1, v/v) to give corresponding pure intermediates 11a–f.

**Intermediate 11a.** The compound was obtained as a yellow solid; yield: 68.8%. <sup>1</sup>H NMR (400 MHz, DMSO): δ 8.43 (s, 1H), 8.04 (dd, J = 8.7, 1.4 Hz, 1H), 7.62 (d, J = 8.7 Hz, 1H), 7.50 (d, J = 7.8 Hz, 1H), 7.45 (d, J = 3.0 Hz, 1H), 7.39 (d, J = 7.5 Hz, 1H), 7.10 (d, J = 7.8 Hz, 1H), 6.61 (d, J = 2.9 Hz, 1H), 3.86 (s, 3H).

**Intermediate 11b.** The compound was obtained as a yellow solid; yield: 49.5%. <sup>1</sup>H NMR (400 MHz, DMSO): δ 7.82 (d, J = 7.3 Hz, 1H), 7.64 (d, J = 8.2 Hz, 1H), 7.57–7.48 (m, 3H), 7.42 (d, J = 7.2 Hz, 1H), 7.34 (t, J = 7.8 Hz, 1H), 7.16 (t, J = 7.8 Hz, 1H), 3.88 (s, 3H).

**Intermediate 11c.** The compound was obtained as a yellow solid; yield: 53.9%. <sup>1</sup>H NMR (400 MHz, DMSO): δ 8.54 (d, J = 7.2 Hz, 1H), 8.13 (s, 1H), 7.57 (d, J = 7.6 Hz, 1H), 7.47 (d, J = 7.8 Hz, 1H), 7.35 (d, J = 7.7 Hz, 1H), 7.32–7.22 (m, 2H), 7.08 (dd, J = 14.3, 6.5 Hz, 1H), 3.92 (s, 3H).

**Intermediate 11d.** The compound was obtained as a yellow solid; yield: 40.3%. <sup>1</sup>H NMR (400 MHz, DMSO): δ 7.79 (d, J = 7.4 Hz, 1H), 7.67 (d, J = 8.1 Hz, 1H), 7.58–7.52 (m, 2H), 7.48 (d, J = 2.9 Hz, 1H), 7.41 (d, J = 7.7 Hz, 1H), 7.31 (s, 1H), 7.15 (t, J = 7.8 Hz, 1H), 4.25 (t, J = 7.0 Hz, 2H), 1.80–1.74 (m, 2H), 1.25 (d, J = 3.8 Hz, 2H), 0.91–0.87 (m, 3H).

**Intermediate 11e.** The compound was obtained as a yellow solid; yield: 60.1%. <sup>1</sup>H NMR (400 MHz, DMSO): δ 8.38 (d, J = 7.3 Hz, 2H), 8.05 (d, J = 8.4 Hz, 2H), 7.62 (d, J = 7.5 Hz, 1H), 7.48 (d, J = 7.6 Hz, 1H), 7.21 (t, J = 7.9 Hz, 1H).

**Intermediate 11f.** The compound was obtained as a yellow solid; yield: 55.7%. <sup>1</sup>H NMR (400 MHz, DMSO): δ 8.60 (s, 1H), 8.52 (d, J = 7.7 Hz, 1H), 7.99 (d, J = 7.7 Hz, 1H), 7.79 (t, J = 7.8 Hz, 1H), 7.62 (d, J = 7.6 Hz, 1H), 7.47 (d, J = 7.7 Hz, 1H), 7.20 (t, J = 7.9 Hz, 1H).

**General Procedures for the Preparation of Compounds 12a–f.** To a solution of intermediate 11a (11b, 11c, 11d, 11e, or 11f) (0.092 mmol) in 4.5 mL of dioxane and 0.5 mL of H<sub>2</sub>O were added (3,4,5-trimethoxyphenyl)boronic acid (23 mg, 0.110 mmol), Na<sub>2</sub>CO<sub>3</sub> (20 mg, 0.184 mmol), and catalytic equivalent of PdCl<sub>2</sub>(dtbpf). The mixture was stirred at 80 °C under a nitrogen atmosphere for 4 h. Then, the solvent was removed *in vacuo*, and the residue was diluted by H<sub>2</sub>O and extracted with EtOAc (3 × 10 mL). The combined organic layer was then washed with brine, dried over anhydrous Na<sub>2</sub>SO<sub>4</sub>, and concentrated *in vacuo* to provide the crude product, which was directly subjected to silica gel column chromatography eluted with petroleum PE/EtOAc (2/1, v/v) to give corresponding pure compounds 12a–f.

**2-(1-Methyl-1H-indole-5-yl)-4-(3,4,5-trimethoxyphenyl)-1H-benzimidazole (12a).** The compound was obtained as a yellow solid; yield: 34.8%. m.p. 182.1–182.7 °C. <sup>1</sup>H NMR (400 MHz, CDCl<sub>3</sub>): δ 8.28 (d, J = 1.1 Hz, 1H), 7.98 (dd, J = 8.6, 1.6 Hz, 1H), 7.68 (dd, J = 6.7, 2.3 Hz, 1H), 7.42 (d, J = 8.6 Hz, 1H), 7.33–7.28 (m, 2H), 7.11 (d, J = 3.1 Hz, 1H), 7.04 (s, 2H), 6.56 (d, J = 3.1 Hz, 1H), 3.94 (s, 6H), 3.93 (s, 3H), 3.83 (s, 3H). HRMS *m/z*: calcd for C<sub>25</sub>H<sub>23</sub>N<sub>3</sub>O<sub>3</sub> [M + H]<sup>+</sup>, 413.1739; found, 414.1859.

**2-(1-Methyl-1H-indole-4-yl)-4-(3,4,5-trimethoxyphenyl)-1H-benzimidazole (12b).** The compound was obtained as a yellow solid; yield: 41.2%. m.p. 181.1–181.5 °C. <sup>1</sup>H NMR (400 MHz, DMSO): δ 7.85 (d, J = 7.4 Hz, 1H), 7.66 (s, 2H), 7.62–7.59 (m, 2H), 7.53–7.50 (m, 3H), 7.38–7.27 (m, 2H), 3.93 (s, 6H), 3.87 (s, 3H), 3.76 (s, 3H). <sup>13</sup>C NMR (101 MHz, DMSO): δ 152.71, 152.00, 141.64, 137.27, 136.99, 135.38, 134.01, 130.73, 130.04, 125.88, 122.67, 121.41, 120.92, 120.02, 118.14, 111.65, 110.27, 106.27, 102.19, 60.16, 55.90, 32.66. HRMS *m/z*: calcd for C<sub>25</sub>H<sub>23</sub>N<sub>3</sub>O<sub>3</sub> [M + H]<sup>+</sup>, 413.1739; found, 414.1888.

**2-(1-Methyl-1H-indole-3-yl)-4-(3,4,5-trimethoxyphenyl)-1H-benzimidazole (12c).** The compound was obtained as a yellow solid; yield: 40.7%. m.p. 182.8–183.0 °C. <sup>1</sup>H NMR (400 MHz, DMSO): δ 8.67 (d, J = 7.8 Hz, 1H), 8.11 (s, 1H), 7.71 (s, 2H), 7.58 (d, J = 8.2 Hz, 1H), 7.49 (d, J = 7.5 Hz, 1H), 7.45 (d, J = 7.9 Hz, 1H), 7.32–7.29 (m, J = 7.3 Hz, 1H), 7.25–7.20 (m, 2H), 3.96 (s, 6H), 3.93 (s, 3H), 3.77 (s, 3H). HRMS *m/z*: calcd for C<sub>25</sub>H<sub>23</sub>N<sub>3</sub>O<sub>3</sub> [M + H]<sup>+</sup>, 413.1739; found, 414.1884.

**2-(1-Butyl-1H-indole-4-yl)-4-(3,4,5-trimethoxyphenyl)-1H-benzimidazole (12d).** The compound was obtained as a yellow solid; yield: 33.6%. m.p. 179.6–180.2 °C. <sup>1</sup>H NMR (400 MHz, DMSO): δ 7.82 (d, J = 7.4 Hz, 1H), 7.65 (d, J = 6.1 Hz, 3H), 7.59 (d, J = 2.8 Hz, 1H), 7.55 (d, J = 3.0 Hz, 1H), 7.51 (dd, J = 7.7, 1.8 Hz, 2H), 7.37–7.24 (m, 2H), 4.24 (t, J = 6.9 Hz, 2H), 3.93 (s, 6H), 3.76 (s, 3H), 1.81–1.73 (m, 2H), 1.30–1.26 (m, 2H), 0.89 (t, J = 7.4 Hz, 3H). HRMS *m/z*: calcd for C<sub>28</sub>H<sub>29</sub>N<sub>3</sub>O<sub>3</sub> [M + H]<sup>+</sup>, 455.2209; found, 456.2357.

**2-(4-Cyanophenyl)-4-(3,4,5-trimethoxyphenyl)-1H-benzimidazole (12e).** The compound was obtained as a yellow solid; yield: 43.5%. m.p. 192.8–193.7 °C. <sup>1</sup>H NMR (400 MHz, DMSO): δ 8.38 (d, J = 8.3 Hz, 2H), 8.05 (d, J = 8.3 Hz, 2H), 7.62–7.55 (m, 3H), 7.55 (d, J = 1.5 Hz, 1H), 7.36 (t, J = 7.8 Hz, 1H), 3.91 (s, 6H), 3.75 (s, 3H). HRMS *m/z*: calcd for C<sub>23</sub>H<sub>19</sub>N<sub>3</sub>O<sub>3</sub> [M + H]<sup>+</sup>, 385.1426; found, 386.1505.

**2-(3-Cyanophenyl)-4-(3,4,5-trimethoxyphenyl)-1H-benzimidazole (12f).** The compound was obtained as a yellow solid; yield: 40.8%. m.p. 191.3–191.8 °C. <sup>1</sup>H NMR (400 MHz, DMSO): δ 8.66–8.49 (m, 2H), 8.01–7.66 (m, 3H), 7.60–7.55 (m, 3H), 7.34 (t, J = 7.5 Hz, 1H), 3.90 (s, 6H), 3.75 (s, 3H). HRMS *m/z*: calcd for C<sub>23</sub>H<sub>19</sub>N<sub>3</sub>O<sub>3</sub> [M + H]<sup>+</sup>, 385.1426; found, 386.1505.

**General Procedures for the Preparation of Compounds 12g and 12h.** To a solution of compound 12e or 12f (30 mg, 0.078 mmol) in 5 mL of anhydrous EtOH were added hydroxylamine hydrochloride (8 mg, 0.117 mmol) and NaHCO<sub>3</sub> (20 mg, 0.156 mmol). The mixture was stirred at 65 °C under a nitrogen atmosphere for 6 h. Then, the solvent was removed *in vacuo*, and the residue was subjected to silica gel column chromatography eluted with petroleum PE/EtOAc (1/2, v/v) to give corresponding pure compound 12g or 12h.

**3-[4-(N-Hydroxycarbamimidoyl)]-5-(3,4,5-trimethoxyphenyl)-1H-indazole (12g).** The compound was obtained as a yellow solid; yield: 51.6%. m.p. 186.7–187.6 °C. <sup>1</sup>H NMR (400 MHz, DMSO): δ 13.08 (s, 1H), 9.79 (s, 1H), 8.20 (d, J = 8.2 Hz, 2H), 7.86 (d, J = 8.2 Hz, 2H), 7.60 (s, 2H), 7.51 (d, J = 7.8 Hz, 2H), 7.30 (t, J = 7.8 Hz, 1H), 5.88 (s, 2H), 3.90 (s, 6H), 3.74 (s, 3H). HRMS *m/z*: calcd for C<sub>23</sub>H<sub>22</sub>N<sub>4</sub>O<sub>4</sub> [M + H]<sup>+</sup>, 418.1641; found, 419.1725.

**3-[3-(N-Hydroxycarbamimidoyl)]-5-(3,4,5-trimethoxyphenyl)-1H-indazole (12h).** The compound was obtained as a yellow solid; yield: 57.2%. m.p. 185.4–185.7 °C. <sup>1</sup>H NMR (400 MHz, DMSO): δ 13.11 (s, 1H), 9.71 (s, 1H), 8.59 (s, 1H), 8.21 (d, J = 7.8 Hz, 1H), 7.77 (d, J = 7.8 Hz, 1H), 7.67 (s, 2H), 7.58 (t, J = 7.8 Hz, 1H), 7.53 (t, J = 7.5 Hz, 2H), 7.33–7.28 (m, 1H), 5.90 (s, 2H), 3.93 (s, 6H), 3.76 (s, 3H). HRMS *m/z*: calcd for C<sub>23</sub>H<sub>22</sub>N<sub>4</sub>O<sub>4</sub> [M + H]<sup>+</sup>, 418.1641; found, 419.1730.

**General Procedures for the Preparation of Compounds 14a–d.** To a solution of intermediate 13 (0.860 mmol) in 9 mL of dioxane and 1 mL of H<sub>2</sub>O were added (3,4,5-trimethoxyphenyl)boronic acid (200 mg, 0.946 mmol), 1-methyl-1H-indole-5-boronic acid (166 mg, 0.946 mmol), Na<sub>2</sub>CO<sub>3</sub> (182 mg, 1.72 mmol), and catalytic equivalent of PdCl<sub>2</sub>(dtbpf). The mixture was stirred at 80 °C under a nitrogen atmosphere for 4 h. Then, the solvent was removed *in vacuo*, and the residue was diluted by H<sub>2</sub>O and extracted with EtOAc (3 × 10 mL). The combined organic layer was then washed with brine, dried over anhydrous Na<sub>2</sub>SO<sub>4</sub>, and concentrated *in vacuo* to provide the crude product, which was subjected to silica gel column chromatography eluted with petroleum PE/EtOAc (4/1, v/v) to give corresponding pure compounds 14a–d.

**3-(1-Methyl-1H-indol-5-yl)-8-(3,4,5-trimethoxyphenyl)imidazo[1,2-a]pyrazine (14a).** The compound was obtained as a white solid; yield: 13.8%. m.p. 162.4–163.2 °C. <sup>1</sup>H NMR (400 MHz, CDCl<sub>3</sub>): δ 8.27 (d, J = 4.6 Hz, 1H), 8.15 (s, 2H), 7.97 (d, J = 4.6 Hz, 1H), 7.92 (s, 1H), 7.86 (s, 1H), 7.53 (d, J = 8.5 Hz, 1H), 7.43 (d, J = 8.4 Hz,

1H), 7.20 (d, *J* = 3.0 Hz, 1H), 6.62 (d, *J* = 3.0 Hz, 1H), 4.05 (s, 6H), 3.98 (s, 3H), 3.91 (s, 3H). HRMS *m/z*: calcd for C<sub>24</sub>H<sub>22</sub>N<sub>4</sub>O<sub>3</sub> [M + H]<sup>+</sup>, 414.1692; found, 415.1816.

**3-(3,4,5-Trimethoxyphenyl)-8-(3,4,5-trimethoxyphenyl)imidazo[1,2-*a*]pyrazine (14b).** The compound was obtained as a white solid; yield: 11.2%. m.p. 165.8–166.8 °C. <sup>1</sup>H NMR (400 MHz, CDCl<sub>3</sub>): δ 8.21 (s, 1H), 8.13 (s, 2H), 8.01 (s, 1H), 7.88 (s, 1H), 6.79 (s, 2H), 4.04 (s, 6H), 3.96 (d, *J* = 3.5 Hz, 12H). <sup>13</sup>C NMR (101 MHz, CDCl<sub>3</sub>): δ 154.04, 153.00, 150.02, 140.21, 139.66, 138.85, 133.74, 131.29, 129.19, 127.11, 123.46, 115.05, 107.08, 105.73, 60.97, 60.87, 56.38, 56.23. HRMS *m/z*: calcd for C<sub>24</sub>H<sub>23</sub>N<sub>3</sub>O<sub>6</sub> [M + H]<sup>+</sup>, 451.1743; found, 452.1835.

**3-(3,4,5-Trimethoxyphenyl)-8-(1-methyl-1H-indol-5-yl)imidazo[1,2-*a*]pyrazine (14c).** The compound was obtained as a white solid; yield: 14.4%. m.p. 166.0–166.3 °C. <sup>1</sup>H NMR (400 MHz, CDCl<sub>3</sub>): δ 9.17 (s, 1H), 8.59 (d, *J* = 8.6 Hz, 1H), 8.18 (s, 1H), 8.03 (s, 1H), 7.92 (s, 1H), 7.51 (d, *J* = 8.6 Hz, 1H), 7.13 (s, 1H), 6.81 (s, 2H), 6.69 (s, 1H), 3.96 (s, 9H), 3.88 (s, 3H). HRMS *m/z*: calcd for C<sub>24</sub>H<sub>22</sub>N<sub>4</sub>O<sub>3</sub> [M + H]<sup>+</sup>, 414.1692; found, 415.1778.

**3-(1-Methyl-1H-indol-5-yl)-8-(1-methyl-1H-indol-5-yl)imidazo[1,2-*a*]pyrazine (14d).** The compound was obtained as a white solid; yield: 16.9%. m.p. 163.9–164.9 °C. <sup>1</sup>H NMR (400 MHz, CDCl<sub>3</sub>): δ 9.20 (s, 1H), 8.62 (d, *J* = 8.5 Hz, 1H), 8.25 (d, *J* = 4.4 Hz, 1H), 8.00 (d, *J* = 4.5 Hz, 1H), 7.97 (s, 1H), 7.88 (s, 1H), 7.52 (t, *J* = 8.1 Hz, 2H), 7.45 (d, *J* = 8.3 Hz, 1H), 7.20 (d, *J* = 3.0 Hz, 1H), 7.13 (d, *J* = 3.0 Hz, 1H), 6.70 (d, *J* = 2.9 Hz, 1H), 6.62 (d, *J* = 2.9 Hz, 1H), 3.91 (s, 3H), 3.88 (s, 3H). HRMS *m/z*: calcd for C<sub>24</sub>H<sub>19</sub>N<sub>5</sub> [M + H]<sup>+</sup>, 377.1640; found, 378.1730.

**Synthesis of Intermediate 21.** To a solution of intermediate 20 (5.0 g, 25.7 mmol) in 15 mL of dimethylformamide (DMF) was added *N,N*-dimethylformamide dimethyl acetal (9.2 g, 77.2 mmol). The mixture was stirred at 120 °C for 6 h, then the reaction was quenched by H<sub>2</sub>O. After being extracted with CH<sub>2</sub>Cl<sub>2</sub> and concentrated *in vacuo*, the crude product was purified by column chromatography to give intermediate 21 as a white solid; yield: 85.4%; <sup>1</sup>H NMR (400 MHz, CDCl<sub>3</sub>): δ 7.65 (d, *J* = 12.3 Hz, 1H), 7.25 (d, *J* = 1.7 Hz, 1H), 7.24 (d, *J* = 1.7 Hz, 1H), 5.53 (d, *J* = 12.3 Hz, 1H), 3.79 (s, 3H), 3.77 (s, 3H), 2.98 (s, 3H), 2.78 (s, 3H), 2.19 (s, 3H).

**Synthesis of Intermediate 22.** To a solution of intermediate 21 (2.0 g, 8.0 mmol) in 10 mL of AcOH was added 3-bromo-1H-pyrazol-5-amine (1.6 g, 9.6 mmol). The mixture was stirred at 80 °C for 8 h. After the completion of the reaction, the cooled mixture was deposited dropwise in H<sub>2</sub>O, and the precipitated solid was filtered and dried to obtain intermediate 22. White solid; yield: 89.5%; <sup>1</sup>H NMR (400 MHz, CDCl<sub>3</sub>): δ 8.52 (d, *J* = 4.4 Hz, 1H), 7.54 (d, *J* = 1.7 Hz, 1H), 7.48 (d, *J* = 1.7 Hz, 1H), 6.92 (d, *J* = 4.4 Hz, 1H), 6.84 (s, 1H), 3.99 (s, 3H), 3.96 (s, 3H), 2.34 (s, 3H).

**General Procedures for the Preparation of Compounds 23a–h.** To a solution of intermediate 22 (117.5 mg, 0.275 mmol) and corresponding boronic acid (0.360 mmol) in 5 mL of DMF and 1 mL of H<sub>2</sub>O, Na<sub>2</sub>CO<sub>3</sub> (73 mg, 0.688 mmol) and Pd(dppf)Cl<sub>2</sub> (10 mg, 0.014 mmol) were added. The mixture was stirred at 95 °C for 12 h, then the reaction was quenched by H<sub>2</sub>O and extracted with CH<sub>2</sub>Cl<sub>2</sub>. The combined organic layers were washed with brine, dried over anhydrous Na<sub>2</sub>SO<sub>4</sub>, and concentrated *in vacuo* to provide the crude product, which was purified by column chromatography with DCM/MeOH (100:1) to give pure compounds 23a–h.

**7-(3,4-Dimethoxy-5-(methylselanyl)phenyl)-2-(1-methyl-1H-indol-5-yl)pyrazolo[1,5-*a*]pyrimidine (23a).** The compound was obtained as a yellow solid; yield: 80.2%; m.p. 156.8–157.7 °C. <sup>1</sup>H NMR (400 MHz, CDCl<sub>3</sub>): δ 8.48 (d, *J* = 4.3 Hz, 1H), 8.31 (s, 1H), 7.96 (d, *J* = 8.5 Hz, 1H), 7.81 (s, 1H), 7.74 (s, 1H), 7.41 (d, *J* = 8.6 Hz, 1H), 7.12 (s, 1H), 7.10 (d, *J* = 3.0 Hz, 1H), 6.89 (d, *J* = 4.3 Hz, 1H), 6.58 (d, *J* = 2.8 Hz, 1H), 4.03 (s, 3H), 4.01 (s, 3H), 3.85 (s, 3H), 2.40 (s, 3H). <sup>13</sup>C NMR (101 MHz, CDCl<sub>3</sub>): δ 157.3, 151.8, 151.3, 148.5, 148.5, 145.3, 137.2, 129.6, 128.7, 128.1, 127.5, 124.2, 121.3, 120.4, 119.3, 111.6, 109.4, 106.2, 101.6, 93.0, 60.1, 56.1, 32.9, 5.2. HRMS *m/z*: calcd for C<sub>24</sub>H<sub>22</sub>N<sub>4</sub>O<sub>2</sub>Se [M + H]<sup>+</sup>, 478.0908; found, 479.0994.

**7-(3,4-Dimethoxy-5-(methylselanyl)phenyl)-2-(*p*-methylphenyl)pyrazolo[1,5-*a*]pyrimidine (23b).** The compound was obtained as a yellow solid; yield: 78.8%; m.p. 152.1–152.9 °C. <sup>1</sup>H NMR (400 MHz, CDCl<sub>3</sub>): δ 8.49 (d, *J* = 4.4 Hz, 1H), 7.93 (d, *J* = 8.0 Hz, 2H), 7.76 (d, *J* = 1.6 Hz, 1H), 7.68 (d, *J* = 1.6 Hz, 1H), 7.29 (d, *J* = 8.0 Hz, 2H), 7.06 (s, 1H), 6.92 (d, *J* = 4.4 Hz, 1H), 4.01 (s, 3H), 3.99 (s, 3H), 2.43 (s, 3H), 2.37 (s, 2H). <sup>13</sup>C NMR (101 MHz, CDCl<sub>3</sub>): δ 155.8, 151.8, 151.2, 148.7, 148.5, 145.5, 138.9, 130.0, 129.4, 128.1, 127.3, 126.3, 121.3, 111.6, 106.6, 93.3, 60.1, 56.1, 21.3, 5.1. HRMS *m/z*: calcd for C<sub>22</sub>H<sub>21</sub>N<sub>3</sub>O<sub>2</sub>Se [M + H]<sup>+</sup>, 439.0799; found, 440.0917.

**7-(3,4-Dimethoxy-5-(methylselanyl)phenyl)-2-(1-methyl-1H-indazol-6-yl)pyrazolo [1,5-*a*]pyrimidine (23c).** The compound was obtained as a yellow solid; yield: 81.6%; m.p. 158.2–159.0 °C. <sup>1</sup>H NMR (400 MHz, CDCl<sub>3</sub>): δ 8.50 (d, *J* = 4.4 Hz, 1H), 8.38 (s, 1H), 8.12 (d, *J* = 8.8, 1H), 8.07 (s, 1H), 7.75 (d, *J* = 1.9 Hz, 1H), 7.70 (d, *J* = 1.9 Hz, 1H), 7.48 (d, *J* = 8.8 Hz, 1H), 7.12 (s, 1H), 6.92 (d, *J* = 4.4 Hz, 1H), 4.13 (s, 3H), 4.02 (s, 3H), 4.00 (s, 3H), 2.38 (s, 3H). <sup>13</sup>C NMR (101 MHz, CDCl<sub>3</sub>): δ 156.1, 151.8, 151.3, 148.8, 148.6, 145.5, 140.1, 133.4, 128.2, 127.3, 125.6, 125.2, 124.3, 121.3, 119.2, 111.5, 109.2, 106.6, 93.2, 60.2, 56.1, 35.6, 5.1. HRMS *m/z*: calcd for C<sub>23</sub>H<sub>21</sub>N<sub>3</sub>O<sub>2</sub>Se [M + H]<sup>+</sup>, 479.0860; found, 480.0962.

**7-(3,4-Dimethoxy-5-(methylselanyl)phenyl)-2-(4-methoxy-3-nitrophenyl)pyrazolo [1,5-*a*]pyrimidine (23d).** The compound was obtained as a yellow solid; yield: 83.5%; m.p. 149.8–150.2 °C. <sup>1</sup>H NMR (400 MHz, CDCl<sub>3</sub>): δ 8.57 (s, 1H), 8.54 (d, *J* = 4.3 Hz, 1H), 8.15 (d, *J* = 8.7 Hz, 1H), 7.75 (s, 1H), 7.65 (s, 1H), 7.20 (d, *J* = 8.7 Hz, 1H), 7.05 (s, 1H), 6.98 (d, *J* = 4.3 Hz, 1H), 4.04 (s, 3H), 4.02 (s, 3H), 4.01 (s, 3H), 2.38 (s, 3H). <sup>13</sup>C NMR (101 MHz, CDCl<sub>3</sub>): δ 153.3, 153.1, 151.9, 151.4, 149.2, 148.8, 145.6, 139.8, 131.9, 128.4, 126.9, 125.8, 123.7, 121.2, 113.7, 111.5, 107.1, 93.3, 60.2, 56.7, 56.1, 5.2. HRMS *m/z*: calcd for C<sub>22</sub>H<sub>20</sub>N<sub>4</sub>O<sub>3</sub>Se [M + H]<sup>+</sup>, 500.0599; found, 501.0684.

**7-(3,4-Dimethoxy-5-(methylselanyl)phenyl)-2-(1H-indol-3-yl)pyrazolo[1,5-*a*]pyrimidine (23e).** The compound was obtained as a yellow solid; yield: 88.7%; m.p. 160.1–161.2 °C. <sup>1</sup>H NMR (400 MHz, CDCl<sub>3</sub>): δ 8.69 (s, 1H), 8.49 (d, *J* = 4.4 Hz, 1H), 8.44 (d, *J* = 8.5 Hz, 1H), 7.83 (d, *J* = 1.5 Hz, 1H), 7.74 (s, 1H), 7.68 (d, *J* = 1.6 Hz, 1H), 7.41 (d, *J* = 8.1 Hz, 1H), 7.29–7.23 (m, 2H), 7.03 (s, 1H), 6.88 (d, *J* = 4.4 Hz, 1H), 4.03 (s, 3H), 4.00 (s, 3H), 2.36 (s, 3H). <sup>13</sup>C NMR (101 MHz, CDCl<sub>3</sub>): δ 152.7, 151.9, 150.7, 148.7, 148.5, 145.4, 136.5, 128.0, 127.8, 125.4, 124.0, 122.7, 121.5, 121.4, 120.7, 111.6, 111.3, 110.4, 106.0, 60.2, 56.1, 5.2. HRMS *m/z*: calcd for C<sub>23</sub>H<sub>20</sub>N<sub>4</sub>O<sub>2</sub>Se [M + H]<sup>+</sup>, 464.0751; found, 465.0847.

**7-(3,4-Dimethoxy-5-(methylselanyl)phenyl)-2-phenylpyrazolo[1,5-*a*]pyrimidine (23f).** The compound was obtained as a yellow solid; yield: 82.9%; m.p. 158.6–159.2 °C. <sup>1</sup>H NMR (400 MHz, CDCl<sub>3</sub>): δ 8.52 (d, *J* = 4.2 Hz, 1H), 8.04 (d, *J* = 7.1 Hz, 2H), 7.76 (d, *J* = 1.9 Hz, 1H), 7.68 (d, *J* = 1.9 Hz, 1H), 7.48 (t, *J* = 7.3 Hz, 2H), 7.42 (t, *J* = 7.3 Hz, 1H), 7.10 (s, 1H), 6.94 (d, *J* = 4.4 Hz, 1H), 4.02 (s, 3H), 4.00 (s, 3H), 2.38 (s, 3H). <sup>13</sup>C NMR (101 MHz, CDCl<sub>3</sub>): δ 155.7, 151.8, 151.2, 148.9, 148.6, 145.6, 132.8, 129.0, 128.7, 128.2, 127.3, 126.4, 121.3, 111.6, 106.8, 93.6, 60.1, 56.1, 5.1. HRMS *m/z*: calcd for C<sub>21</sub>H<sub>19</sub>N<sub>3</sub>O<sub>2</sub>Se [M + H]<sup>+</sup>, 425.0642; found, 426.0746.

**7-(3,4-Dimethoxy-5-(methylselanyl)phenyl)-2-(1-hydroxymethyl-1H-indole-3-yl)pyrazolo [1,5-*a*]pyrimidine (23g).** The compound was obtained as a yellow solid; yield: 80.6%; m.p. 150.3–151.6 °C. <sup>1</sup>H NMR (400 MHz, methanol-*d*<sub>4</sub>): δ 8.41 (d, *J* = 4.5 Hz, 1H), 8.36 (d, *J* = 7.8 Hz, 1H), 7.81 (s, 1H), 7.76 (d, *J* = 1.7 Hz, 1H), 7.67 (d, *J* = 1.7 Hz, 1H), 7.55 (d, *J* = 8.1 Hz, 1H), 7.28 (t, *J* = 7.3 Hz, 1H), 7.21 (t, *J* = 7.4 Hz, 1H), 6.97 (s, 1H), 6.90 (d, *J* = 4.5 Hz, 1H), 5.63 (s, 2H), 3.98 (s, 3H), 3.97 (s, 3H), 2.33 (s, 3H). <sup>13</sup>C NMR (101 MHz, CD<sub>3</sub>OD): δ 152.9, 151.8, 150.2, 148.6, 148.4, 145.9, 136.4, 128.1, 127.6, 127.5, 126.4, 122.6, 121.5, 121.3, 120.8, 111.5, 109.9, 109.5, 106.0, 92.3, 69.3, 60.0, 55.9, 4.8. HRMS *m/z*: calcd for C<sub>24</sub>H<sub>22</sub>N<sub>4</sub>O<sub>3</sub>Se [M + H]<sup>+</sup>, 494.0857; found, 495.0949.

**7-(3,4-Dimethoxy-5-(methylselanyl)phenyl)-2-(4-(methylsulfonyl)phenyl)pyrazolo [1,5-*a*]pyrimidine (23h).** The compound was obtained as a yellow solid; yield: 85.6%; m.p. 156.6–157.7 °C. <sup>1</sup>H NMR (400 MHz, CDCl<sub>3</sub>): δ 8.56 (d, *J* = 4.1 Hz, 1H), 8.21 (d, *J* = 8.2 Hz, 2H), 8.04 (d, *J* = 8.2 Hz, 2H), 7.69 (s, 1H),

7.65 (s, 1H), 7.17 (s, 1H), 7.00 (d,  $J = 4.1$  Hz, 1H), 4.02 (s, 3H), 3.98 (s, 3H), 3.11 (s, 3H), 2.36 (s, 3H).  $^{13}\text{C}$  NMR (101 MHz,  $\text{CDCl}_3$ ):  $\delta$  153.4, 151.9, 151.3, 149.4, 148.8, 145.9, 140.4, 138.2, 128.4, 127.9, 127.1, 126.8, 121.2, 111.5, 107.6, 94.6, 60.2, 56.1, 44.5, 5.1. HRMS  $m/z$ : calcd for  $\text{C}_{22}\text{H}_{21}\text{N}_3\text{O}_4\text{SSe} [\text{M} + \text{H}]^+$ , 503.0418; found, 504.0492.

**Biological Assays. Cell Lines and Cell Culture.** The cancer cell lines were purchased from American Type Culture Collection (ATCC). Human breast cancer cells (MCF-7) and human lung cancer cells (A549) were grown in RPMI-1640 medium (Life Technologies, USA). Human cervical cancer cells and murine melanoma cells were grown in Dulbecco's modified Eagle's medium (Life Technologies, USA). The medium for all cell lines was supplemented with 10% fetal bovine serum (Life Technologies, USA) and 1% penicillin–streptomycin (Life Technologies, USA) and maintained at 37 °C in a humidified atmosphere with 5%  $\text{CO}_2$ .

**Cytotoxicity Assay.** The cytotoxicity of the test compounds was evaluated against MCF-7, A549, HeLa, B16-F10, A2780S, and A2780/T using the MTT assay. Cells were seeded into 96-well plates at a density of 5000 cells/well. After removing the medium, 100  $\mu\text{L}$  of medium with 0.1% DMSO containing our antitubulin compounds at different concentrations was added to each well and incubated at 37 °C for another 48 h. The MTT (5 mg/mL in PBS) was added and incubated for another 4 h, and then, the absorbance was detected with a microplate reader at a wavelength of 570 nm. The  $\text{IC}_{50}$  values were calculated by nonlinear regression analysis using GraphPad Prism. All the experiments were repeated in at least three independent experiments.

**In Vitro Antiproliferative Assay.** Cells were seeded into 96-well plates at a density of 5000 cells/well. After being treated with compound **12b** at the indicated concentrations or time points, the MTT (5 mg/mL in PBS) was added and incubated for another 4 h. Cell viability was detected with a microplate reader at a wavelength of 570 nm.

**Colony Formation Assay.** MCF-7 cells (1000 units) were counted and seeded in 6-well plates. After being cultured for 24 h at 37 °C, the medium was replaced with medium added with compound **12b** at the indicated concentration. After 24 h treatment, the medium was changed to normal. After being cultured for another 10–14 days, the colonies were fixed with 4% paraformaldehyde for 30 min and stained with 0.1% crystal violet for 15 min. Following washing with PBS, the colonies were then photographed and quantified using Image J.

**In Vitro Tubulin Polymerization Assay.** Pig brain microtubule protein was isolated *via* three cycles of temperature-dependent assembly/disassembly in 100 mM PIPES (pH 6.5), 1 mM GTP, 1 mM  $\text{MgSO}_4$ , 2 mM EGTA, and 1 mM 2-mercaptoethanol. Glycerol and phenylmethylsulfonyl fluoride were added in 4 M and 0.2 mM, respectively, in the first cycle of polymerization. Tubulin was prepared from microtubule protein by phosphocellulose (P11) chromatography, stored at –70 °C. Tubulin was mixed with different concentrations of compounds in PEM buffer (100 mM PIPES, 1 mM  $\text{MgCl}_2$ , and 1 mM EGTA) containing 1 mM GTP and 5% glycerol. Microtubule polymerization was detected by a spectrophotometer at 340 nm at 37 °C. The plateau absorbance values were used for calculations.

**Immunofluorescence Staining.** B16-F10 cells were seeded on glass coverslips in 24-well plates and then treated with vehicle control 0.1% DMSO, **12b** (10, 20, 40 nM) for 6 h. The cells were fixed with 4% paraformaldehyde and then penetrated with PBS containing 0.2% Triton X-100. After blocking for 30 min by adding 100  $\mu\text{L}$  of goat serum albumin at room temperature, cells were incubated with a monoclonal antibody (anti- $\beta$ -tubulin) at 37 °C for 1 h. Then, the cells were washed three times by PBS following staining by the fluorescence secondary antibody. Nuclei were labeled by 4,6-diamidino-2-phenylindole (DAPI). Cells were finally visualized using a fluorescence microscope.

**Cell Cycle Analysis.** MCF-7 cells were seeded into 6-well plates and cultured overnight. Cells were treated with **12b** (5, 10, and 20 nM) for 48 h. The collected cells were fixed at 4 °C with 70% ethanol overnight. The fixed cells were washed and resuspended using PBS with 10 mg/mL RNaseA and 50 mg/mL PI. After that, samples were

incubated for 30 min in the dark. Then, samples were analyzed for the DNA content with flow cytometry (BD FACSCanto II).

**Analysis of Cancer Cell Apoptosis.** MCF-7 cells were seeded into 6-well plates and cultured overnight. After treating with **12b** (5, 10, and 20 nM) for 48 h, cells were harvested and suspended in binding buffer containing annexin V-FITC (0.5 mg/mL) and PI (0.5 mg/mL). After that, samples were incubated for 30 min in the dark and analyzed with a flow cytometer (BD FACSCanto II).

**Wound Healing Assay.** B16-F10 cells were seeded and incubated in a 6-well plates overnight. Scratches were made in confluent monolayers by a 200  $\mu\text{L}$  pipette tip. Then, wounds were washed twice with media to remove debris and uprooted cells. Cells were treated with different concentrations (0, 5, 10, and 20 nM) of compound **12b**. Images were obtained using phase contrast microscopy at 0 and 24 h. The migration distance of cells in the wound area was measured manually.

**In Vivo Antitumor Evaluation.** The animal experiments were performed with the approval of the National Institutional Animal Care and Use Committee (IACUC) of Southern Medical University. Male BALB/c mice, 6–8 weeks old, purchased from SPF (Beijing) Biotechnology Co. Ltd., were used to study the inhibition effect of compound **12b** on the subcutaneous transplanted model of melanoma cells. Logarithmic growth phase B16-F10 cells ( $4 \times 10^6$  per mL) were suspended in PBS before injecting into mice. Tumors were established by inoculating subcutaneously with 200  $\mu\text{L}$  containing  $8 \times 10^5$  cells into each mouse. Mice were divided into control or treatment groups ( $n = 8$ ) randomly. Compound **12b** or paclitaxel was dissolved in a 1:1 ratio of PEG300/PBS solution to produce the desired concentrations. The vehicle control solution was formulated with equal parts PEG300 and PBS only. Dose of the drug treatment (paclitaxel, 10 mg/kg; compound **12b**, 15, 30 mg/kg) or vehicle control was administered *via* i.p. injection every day once for 14 days. Body weight was monitored during the entire experiment period to assess acute toxicity. Tumor volume was measured with a caliper and calculated using the formula  $a \times b^2 \times 0.5$ , where  $a$  and  $b$  represent the larger and smaller diameters, respectively. Mice were sacrificed 14 days after the initiation of the experiment, and the tumors were weighed. The TGI value was calculated using the formula:  $\text{TGI} (\%) = [1 - W_t/W_v] \times 100\%$ , where  $W_t$  and  $W_v$  are the mean tumor weight of the treatment group and vehicle control. The harvested organs (liver and kidney) were fixed in 4% paraformaldehyde, processed into paraffin routinely, stained with H&E, and captured by the microscope.

**Protein Expression and Purification.** TTL protein was expressed and purified from *Escherichia coli*, as described by Prota *et al.* (2013)<sup>44</sup> and Wang *et al.* (2016).<sup>45</sup> The stathmin-like domain of RB3 (RB3-SLD) and TTL recombinant plasmids were transformed into *E. coli* strain BL21(DE3) (TransGen Biotech) for protein expression. The bacterial cells were grown in Luria broth supplemented with antibiotic at 37 °C. RB3-SLD protein was induced by the addition of 0.4 mM isopropyl- $\beta$ -D-thiogalactoside at 37 °C for 3 h. Cells were collected and sonicated in lysis buffer (20 mM Tris pH 8.0, 200 mM NaCl, 1 mM EDTA, 2 mM DTT, and 1 mM PMSF). Then, the protein was purified *via* anion-exchange chromatography and gel filtration chromatography. TTL was concentrated to 20 mg/mL and stored at –80 °C.

**Crystallization, Data Collection, and Processing.** Detailed process to obtain crystals of T2R-TTL was described by Prota *et al.* (2013)<sup>44</sup> and Wang *et al.* (2017).<sup>46</sup> The T2R-TTL complex was formed by mixing tubulin, RB3-SLD, and TTL at a 2:1.3:1.2 molar ratio. Then, 5 mM tyrosine, 10 mM DTT, and 1 mM AMPPCP were added, and the complex was concentrated to 20 mg/mL at 4 °C. Protein crystallization trials were performed using 1  $\mu\text{L}$  of protein mixed with 1  $\mu\text{L}$  of reservoir solution at 16 °C. Crystals appeared after incubation at 16 °C and formed rodlike crystals within 3–5 days. A volume of 0.1  $\mu\text{L}$  of compound **12b**, dissolved in 10 mM dimethylsulfoxide, was added to a sitting drop containing crystals at 16 °C for soaking for 4 h. For data collection, all crystals were cryo-protected by briefly soaking in reservoir solution supplemented with 20% (v/v) glycerol before flash-cooling in liquid nitrogen. Structures were solved by molecular replacement with Phaser<sup>47</sup> using the T2R-

TTL structure (PDB ID: 7DBA) as template. The initial models were refined alternating cycles of automatic refinement with Refmac5<sup>48</sup> in CCP4 program suite and manual model building with Coot.<sup>49</sup> The model quality checked with the PROCHECK program shows a good stereochemistry, according to the Ramachandran plot.<sup>50</sup> PYMOL (<http://www.pymol.org>) was used to generate the figures.

## ■ ASSOCIATED CONTENT

### SI Supporting Information

The Supporting Information is available free of charge at <https://pubs.acs.org/doi/10.1021/acs.jmedchem.0c01837>.

Colony formation assay on A2780T cells, binding kinetics of compound **12b** to tubulin (T2R-TTL), binding poses for colchicine and compound **12b** in tubulin (PDB code: 7DBA), *in vitro* metabolic stability studies, HRMS, infrared, <sup>1</sup>H NMR, <sup>13</sup>C NMR, and HPLC (PDF)

Molecular formula strings (CSV)

## ■ AUTHOR INFORMATION

### Corresponding Author

Jianjun Chen – School of Pharmaceutical Sciences, Guangdong Provincial Key Laboratory of New Drug Screening, Southern Medical University, Guangzhou 510515, China; [orcid.org/0000-0001-5668-6572](https://orcid.org/0000-0001-5668-6572); Email: [jchen21@smu.edu.cn](mailto:jchen21@smu.edu.cn)

### Authors

Yichang Ren – School of Pharmaceutical Sciences, Guangdong Provincial Key Laboratory of New Drug Screening, Southern Medical University, Guangzhou 510515, China

Yuxi Wang – Targeted Tracer Research and Development Laboratory, Precision Medicine Research Center, Department of Respiratory and Critical Care Medicine, West China Hospital, Sichuan University, Chengdu 610041, China

Gang Li – Guangdong Key Laboratory of Animal Conservation and Resource Utilization, Guangdong Public Laboratory of Wild Animal Conservation and Utilization, Institute of Zoology, Guangdong Academy of Sciences, Guangzhou 510260, China; [orcid.org/0000-0003-4191-7643](https://orcid.org/0000-0003-4191-7643)

Zherong Zhang – Department of Psychological and Brain Sciences, Dartmouth College, Hanover, New Hampshire 03755, United States

Lingling Ma – Targeted Tracer Research and Development Laboratory, Precision Medicine Research Center, Department of Respiratory and Critical Care Medicine, West China Hospital, Sichuan University, Chengdu 610041, China

Binbin Cheng – School of Pharmaceutical Sciences, Guangdong Provincial Key Laboratory of New Drug Screening, Southern Medical University, Guangzhou 510515, China

Complete contact information is available at: <https://pubs.acs.org/doi/10.1021/acs.jmedchem.0c01837>

### Author Contributions

<sup>†</sup>Y.R., Y.W., and G.L. contributed equally.

### Notes

The authors declare no competing financial interest.

## ■ ACKNOWLEDGMENTS

We thank Dr. Benoît Gigant [Institute for Integrative Biology of the Cell (I2BC), CEA, CNRS, Univ. Paris-Sud, Université Paris-Saclay, France] and Dr. Michel O. Steinmetz (Paul Scherrer Institute, Switzerland) for kindly providing the plasmids of RB3-SLD and TTL. We also thank Jianjian Zhou of Beijing Loham Trading Co. Ltd. for SPR assistance. This work was supported by the scientific research project of high-level talents (no. G618319142) in Southern Medical University of China; International Science and Technology Cooperation Projects of Guangdong Province (no. G819310411); Thousand Youth Talents Program (no. C1080092) from the Organization Department of the CPC Central Committee, China; GDAS Special Project of Science and Technology Development (2016GDASRC-0104 and 2018GDASCX-0107); and Guangdong Basic Research Foundation (no. 2019A1515110616). The X-ray work was supported by the National Major Scientific and Technological Special Project for “Significant New Drugs Development” (no. 2018ZX09201018-021), National Natural Science Foundation of China (no. 81703553), China Postdoctoral Science Foundation (nos. 2017M610607 and 2018T110984), and Sichuan Science and Technology Program (no. 2019YFS0003).

## ■ ABBREVIATIONS

ABI, 2-aryl-4-benzoyl-imidazoles; ABP, 6-aryl-2-benzoyl-pyridine/phenyl; CBSIs, colchicine-binding site inhibitors; H&E, hematoxylin and eosin; HRMS, high-resolution mass spectrometry; MDR, multi-drug resistance; MTAs, microtubule-targeting agents; P-gp, P-glycoprotein; RI, resistance index; SAI, substituted-2-aryl imidazoles; SMART, 4-substituted methoxybenzoyl-aryl-thiazoles; SPR, surface plasmon resonance; TGI, tumor growth inhibition; TMP, trimethoxyphenyl

## ■ REFERENCES

- (1) Knossow, M.; Campanacci, V.; Khodja, L. A.; Gigant, B. The mechanism of tubulin assembly into microtubules: insights from structural studies. *iScience* **2020**, *23*, 101511.
- (2) Nogales, E. Structural insights into microtubule function. *Annu. Rev. Biochem.* **2000**, *69*, 277–302.
- (3) Karahalil, B.; Yardım-Akaydin, S.; Nacak Baytas, S. An overview of microtubule targeting agents for cancer therapy. *Arh. Hig. Rada Toksikol.* **2019**, *70*, 160–172.
- (4) Čermák, V.; Dostál, V.; Jelínek, M.; Libusová, L.; Kovář, J.; Rösel, D.; Brábek, J. Microtubule-targeting agents and their impact on cancer treatment. *Eur. J. Cell Biol.* **2020**, *99*, 151075.
- (5) Heald, R.; Nogales, E. Microtubule dynamics. *J. Cell Sci.* **2002**, *115*, 3–4.
- (6) Parness, J.; Horwitz, S. Taxol binds to polymerized tubulin *in vitro*. *J. Cell Biol.* **1981**, *91*, 479–487.
- (7) Nogales, E.; Grayer Wolf, S.; Khan, I. A.; Ludueña, R. F.; Downing, K. H. Structure of tubulin at 6.5 Å and location of the taxol-binding site. *Nature* **1995**, *375*, 424–427.
- (8) Gigant, B.; Wang, C.; Ravelli, R. B. G.; Roussi, F.; Steinmetz, M. O.; Curmi, P. A.; Sobel, A.; Knossow, M. Structural basis for the regulation of tubulin by vinblastine. *Nature* **2005**, *435*, 519–522.
- (9) Ranaivoson, F. M.; Gigant, B.; Berritt, S.; Joulié, M.; Knossow, M. Structural plasticity of tubulin assembly probed by vinca-domain ligands. *Acta Crystallogr., Sect. D: Biol. Crystallogr.* **2012**, *68*, 927–934.
- (10) Pryor, D. E.; O’Brate, A.; Bilcer, G.; Díaz, J. F.; Wang, Y.; Wang, Y.; Kabaki, M.; Jung, M. K.; Andreu, J. M.; Ghosh, A. K.; Giannakakou, P.; Hamel, E. The Microtubule Stabilizing Agent Laulimalide Does Not Bind in the Taxoid Site, Kills Cells Resistant to

Paclitaxel and Epothilones, and May Not Require Its Epoxide Moiety for Activity†. *Biochemistry* **2002**, *41*, 9109–9115.

(11) Prota, A. E.; Bargsten, K.; Northcote, P. T.; Marsh, M.; Altmann, K.-H.; Miller, J. H.; Díaz, J. F.; Steinmetz, M. O. Structural basis of microtubule stabilization by laulimalide and peloruside A. *Angew. Chem., Int. Ed. Engl.* **2014**, *53*, 1621–1625.

(12) Prota, A. E.; Setter, J.; Waight, A. B.; Bargsten, K.; Murga, J.; Diaz, J. F.; Steinmetz, M. O. Pironetin Binds Covalently to  $\alpha$ Cys316 and Perturbs a Major Loop and Helix of  $\alpha$ -Tubulin to Inhibit Microtubule Formation. *J. Mol. Biol.* **2016**, *428*, 2981–2988.

(13) Prota, A. E.; Bargsten, K.; Diaz, J. F.; Marsh, M.; Cuevas, C.; Liniger, M.; Neuhaus, C.; Andreu, J. M.; Altmann, K.-H.; Steinmetz, M. O. A new tubulin-binding site and pharmacophore for microtubule-destabilizing anticancer drugs. *Proc. Natl. Acad. Sci. U.S.A.* **2014**, *111*, 13817–13821.

(14) Menchon, G.; Prota, A. E.; Lucena-Agell, D.; Bucher, P.; Jansen, R.; Irschik, H.; Muller, R.; Paterson, I.; Diaz, J. F.; Altmann, K. H.; Steinmetz, M. O. A fluorescence anisotropy assay to discover and characterize ligands targeting the maytansine site of tubulin. *Nat. Commun.* **2018**, *9*, 2106.

(15) Ravelli, R. B. G.; Gigant, B.; Curmi, P. A.; Jourdain, I.; Lachkar, S.; Sobel, A.; Knossow, M. Insight into tubulin regulation from a complex with colchicine and a stathmin-like domain. *Nature* **2004**, *428*, 198–202.

(16) Gaspari, R.; Prota, A. E.; Bargsten, K.; Cavalli, A.; Steinmetz, M. O. Structural Basis of cis - and trans -Combretastatin Binding to Tubulin. *Chem* **2017**, *2*, 102–113.

(17) Mosca, L.; Ilari, A.; Fazi, F.; Assaraf, Y. G.; Colotti, G. Taxanes in cancer treatment: activity, chemoresistance and its overcoming. *Drug Resist. Updates* **2021**, *54*, 100742.

(18) Martino, E.; Casamassima, G.; Castiglione, S.; Cellupica, E.; Pantalone, S.; Papagni, F.; Rui, M.; Siciliano, A. M.; Collina, S. Vinca alkaloids and analogues as anti-cancer agents: looking back, peering ahead. *Bioorg. Med. Chem. Lett.* **2018**, *28*, 2816–2826.

(19) Sai, S.; Toyoda, M.; Tobimatsu, K.; Satake, H.; Yasui, H.; Kimbara, S.; Koyama, T.; Fujishima, Y.; Imamura, Y.; Funakoshi, Y.; Kiyota, N.; Toyama, H.; Kodama, Y.; Minami, H. Phase I study of Gemcitabine/Nab-paclitaxel/S-1 in patients with unresectable pancreatic cancer (GeNeSIS trial). *Cancer Chemother. Pharmacol.* **2021**, *87*, 65–71.

(20) Fojo, A. T.; Menefee, M. Microtubule targeting agents: basic mechanisms of multidrug resistance (MDR). *Semin. Oncol.* **2005**, *32*, S3–S8.

(21) Perez, E. A. Microtubule inhibitors: differentiating tubulin-inhibiting agents based on mechanisms of action, clinical activity, and resistance. *Mol. Cancer Ther.* **2009**, *8*, 2086–2095.

(22) Mohr, L.; Carceles-Cordon, M.; Woo, J.; Cordon-Cardo, C.; Domingo-Domenech, J.; Rodriguez-Bravo, V. Generation of prostate cancer cell models of resistance to the anti-mitotic agent Docetaxel. *J. Visualized Exp.* **2017**, *127*, 56327.

(23) Maloney, S. M.; Hoover, C. A.; Morejon-Lasso, L. V.; Prosperi, J. R. Mechanisms of taxane resistance. *Cancers* **2020**, *12*, 3323.

(24) Bai, Z.; Gao, M.; Zhang, H.; Guan, Q.; Xu, J.; Li, Y.; Qi, H.; Li, Z.; Zuo, D.; Zhang, W.; Wu, Y. BZML, a novel colchicine binding site inhibitor, overcomes multidrug resistance in A549/Taxol cells by inhibiting P-gp function and inducing mitotic catastrophe. *Cancer Lett.* **2017**, *402*, 81–92.

(25) Li, W.; Sun, H.; Xu, S.; Zhu, Z.; Xu, J. Tubulin inhibitors targeting the colchicine binding site: a perspective of privileged structures. *Future Med. Chem.* **2017**, *9*, 1765–1794.

(26) Arnst, K. E.; Wang, Y.; Hwang, D.-J.; Xue, Y.; Costello, T.; Hamilton, D.; Chen, Q.; Yang, J.; Park, F.; Dalton, J. T.; Miller, D. D.; Li, W. A potent, metabolically stable tubulin inhibitor targets the colchicine binding site and overcomes taxane resistance. *Cancer Res.* **2018**, *78*, 265–277.

(27) McLoughlin, E. C.; O'Boyle, N. M. Colchicine-binding site inhibitors from chemistry to clinic: a review. *Pharmaceuticals* **2020**, *13*, 8.

(28) Chen, J.; Ahn, S.; Wang, J.; Lu, Y.; Dalton, J. T.; Miller, D. D.; Li, W. Discovery of novel 2-aryl-4-benzoyl-imidazole (ABI-III) analogues targeting tubulin polymerization as antiproliferative agents. *J. Med. Chem.* **2012**, *55*, 7285–7289.

(29) Deng, S.; Krutilina, R. I.; Wang, Q.; Lin, Z.; Parke, D. N.; Playa, H. C.; Chen, H.; Miller, D. D.; Seagroves, T. N.; Li, W. An orally available tubulin inhibitor, VERU-111, suppresses triple-negative breast cancer tumor growth and metastasis and bypasses taxane resistance. *Mol. Cancer Ther.* **2020**, *19*, 348–363.

(30) Lu, Y.; Li, C.-M.; Wang, Z.; Ross, C. R., 2nd; Chen, J.; Dalton, J. T.; Li, W.; Miller, D. D. Discovery of 4-Substituted Methoxybenzoyl-aryl-thiazole as Novel Anticancer Agents: Synthesis, Biological Evaluation, and Structure–Activity Relationships. *J. Med. Chem.* **2009**, *52*, 1701–1711.

(31) Li, L.; Quan, D.; Chen, J.; Ding, J.; Zhao, J.; Lv, L.; Chen, J. Design, synthesis, and biological evaluation of 1-substituted -2-aryl imidazoles targeting tubulin polymerization as potential anticancer agents. *Eur. J. Med. Chem.* **2019**, *184*, 111732.

(32) Li, C.-M.; Chen, J.; Lu, Y.; Narayanan, R.; Parke, D. N.; Li, W.; Ahn, S.; Miller, D. D.; Dalton, J. T. Pharmacokinetic optimization of 4-substituted methoxybenzoyl-aryl-thiazole and 2-aryl-4-benzoyl-imidazole for improving oral bioavailability. *Drug Metab. Dispos.* **2011**, *39*, 1833–1839.

(33) Wang, Q.; Arnst, K. E.; Wang, Y.; Kumar, G.; Ma, D.; Chen, H.; Wu, Z.; Yang, J.; White, S. W.; Miller, D. D.; Li, W. Structural modification of the 3,4,5-trimethoxyphenyl moiety in the tubulin inhibitor VERU-111 leads to improved antiproliferative activities. *J. Med. Chem.* **2018**, *61*, 7877–7891.

(34) Wang, Q.; Arnst, K. E.; Wang, Y.; Kumar, G.; Ma, D.; White, S. W.; Miller, D. D.; Li, W.; Li, W. Structure-Guided Design, Synthesis, and Biological Evaluation of (2-(1H-Indol-3-yl)-1H-imidazol-4-yl)-(3,4,5-trimethoxyphenyl) Methanone (ABI-231) Analogues Targeting the Colchicine Binding Site in Tubulin. *J. Med. Chem.* **2019**, *62*, 6734–6750.

(35) Chen, H.; Deng, S.; Wang, Y.; Albadari, N.; Kumar, G.; Ma, D.; Li, W.; White, S. W.; Miller, D. D.; Li, W. Structure-activity relationship study of novel 6-aryl-2-benzoyl-pyridines as tubulin polymerization inhibitors with potent antiproliferative properties. *J. Med. Chem.* **2020**, *63*, 827–846.

(36) Zhai, M.; Wang, L.; Liu, S.; Wang, L.; Yan, P.; Wang, J.; Zhang, J.; Guo, H.; Guan, Q.; Bao, K.; Wu, Y.; Zhang, W. Synthesis and biological evaluation of (1-aryl-1H-pyrazol-4-yl) (3,4,5-trimethoxyphenyl)methanone derivatives as tubulin inhibitors. *Eur. J. Med. Chem.* **2018**, *156*, 137–147.

(37) Pang, Y.; An, B.; Lou, L.; Zhang, J.; Yan, J.; Huang, L.; Li, X.; Yin, S. Design, synthesis, and biological evaluation of novel selenium-containing isocombretastatins and phenstatins as antitumor agents. *J. Med. Chem.* **2017**, *60*, 7300–7314.

(38) Zhang, S.; An, B.; Li, J.; Hu, J.; Huang, L.; Li, X.; Chan, A. S. C. Synthesis and evaluation of selenium-containing indole chalcone and diarylketone derivatives as tubulin polymerization inhibition agents. *Org. Biomol. Chem.* **2017**, *15*, 7404–7410.

(39) Hwang, D.-J.; Wang, J.; Li, W.; Miller, D. D. Structural optimization of indole derivatives acting at colchicine binding site as potential anticancer agents. *ACS Med. Chem. Lett.* **2015**, *6*, 993–997.

(40) Xu, Q.; Sun, M.; Bai, Z.; Wang, Y.; Wu, Y.; Tian, H.; Zuo, D.; Guan, Q.; Bao, K.; Wu, Y.; Zhang, W. Design, synthesis and bioevaluation of antitubulin agents carrying diaryl-5,5-fused-heterocycle scaffold. *Eur. J. Med. Chem.* **2017**, *139*, 242–249.

(41) Beck, D. E.; Abdelmalak, M.; Lv, W.; Reddy, P. V. N.; Tender, G. S.; O'Neill, E.; Agama, K.; Marchand, C.; Pommier, Y.; Cushman, M. Discovery of potent indenoisoquinoline topoisomerase I poisons lacking the 3-nitro toxicophore. *J. Med. Chem.* **2015**, *58*, 3997–4015.

(42) Guo, W.; Dong, W.; Li, M.; Shen, Y. Mitochondria P-glycoprotein confers paclitaxel resistance on ovarian cancer cells. *Oncotargets Ther.* **2019**, *12*, 3881–3891.

(43) Thanassavate, B.; Ngwisara, L.; Lirdpramongkol, K.; Svasti, J.; Chuawong, P. A synthetic 2,3-diarylindole induces

microtubule destabilization and G2/M cell cycle arrest in lung cancer cells. *Bioorg. Med. Chem. Lett.* **2020**, *30*, 126777.

(44) Prota, A. E.; Bargsten, K.; Zurwerra, D.; Field, J. J.; Díaz, J. F.; Altmann, K.-H.; Steinmetz, M. O. Molecular mechanism of action of microtubule-stabilizing anticancer agents. *Science* **2013**, *339*, 587–590.

(45) Wang, Y.; Zhang, H.; Gigant, B.; Yu, Y.; Wu, Y.; Chen, X.; Lai, Q.; Yang, Z.; Chen, Q.; Yang, J. Structures of a diverse set of colchicine binding site inhibitors in complex with tubulin provide a rationale for drug discovery. *FEBS J.* **2016**, *283*, 102–111.

(46) Wang, Y.; Yu, Y.; Li, G. B.; Li, S. A.; Wu, C.; Gigant, B.; Qin, W.; Chen, H.; Wu, Y.; Chen, Q.; Yang, J. Mechanism of microtubule stabilization by taccalonolide AJ. *Nat. Commun.* **2017**, *8*, 15787.

(47) McCoy, A. J.; Grosse-Kunstleve, R. W.; Adams, P. D.; Winn, M. D.; Storoni, L. C.; Read, R. J. Phaser crystallographic software. *J. Appl. Crystallogr.* **2007**, *40*, 658–674.

(48) Murshudov, G. N.; Skubák, P.; Lebedev, A. A.; Pannu, N. S.; Steiner, R. A.; Nicholls, R. A.; Winn, M. D.; Long, F.; Vagin, A. A. REFMAC5 for the refinement of macromolecular crystal structures. *Acta Crystallogr., Sect. D: Biol. Crystallogr.* **2011**, *67*, 355–367.

(49) Emsley, P.; Cowtan, K. Coot: model-building tools for molecular graphics. *Acta Crystallogr., Sect. D: Biol. Crystallogr.* **2004**, *60*, 2126–2132.

(50) Laskowski, R. A.; Rullmann, J. A.; MacArthur, M. W.; Kaptein, R.; Thornton, J. M. AQUA and PROCHECK-NMR: programs for checking the quality of protein structures solved by NMR. *J. Biomol. NMR* **1996**, *8*, 477–486.